OLFACTORY DISPLAY FOR THE TREADPORT ACTIVE WIND TUNNEL

by

Price Lefler

A thesis submitted to the faculty of
The University of Utah
in partial fulfillment of the requirements for the degree of

Master of Science

Department of Mechanical Engineering

The University of Utah

August 2012

THE UNIVERSITY OF UTAH GRADUATE SCHOOL

STATEMENT OF THESIS APPROVAL

The thesis of **Price Lefler**

has been approved by the following supervisory committee members:

Mark Minor	, Chair	**4/23/12** Date Approved
John Hollerbach	, Member	**1/9/12** Date Approved
Eric Pardyjak	, Member	**1/9/12** Date Approved

and by **Timothy Ameel** , Chair of

the Department of **Mechanical Engineering**

and by Charles A. Wight, Dean of The Graduate School.

ABSTRACT

This thesis discusses the development of an olfactory display for the University of Utah TreadPort Virtual Environment (UUTVE). The goal of the UUTVE is to create a virtual environment that is as life like as possible by communicating to the user as many of the sensations felt in moving around in real the world as possible, while staying within the confines of the virtual environment's workspace. The UUTVE has a visual display, auditory display, a locomotion interface and wind display. With the wind display, it is possible to create an effective olfactory display that does not have some of the limitations associated with many of the current olfactory displays.

The inclusion of olfactory information in virtual environments is becoming increasingly common as the effects of including an olfactory display show an increase in user presence. The development of the olfactory display for the UUTVE includes the following components: the physical apparatus for injecting scent particles into the air stream, the development of a Computational Fluid Dynamics (CFD) model with which to control the concentration of scent being sensed by the user, and user studies to verify the model and show as proof of concept that the wind tunnel can be used to create an olfactory display. The physical apparatus of the display consists of air atomizing nozzles, solenoids for controlling when the scents are released, containers for holding the scents and a pressurized air tank used to provide the required air to make the nozzles work. CFD

is used model the wind flow through the TPAWT. The model of the wind flow is used to simulate how particles advect in the wind tunnel. These particle dispersion simulations are then used to create a piecewise model that is able to predict the scent's concentration behavior as the odor flows through the wind tunnel. The user studies show that the scent delivery system is able to display an odor to a person standing in the TPAWT. The studies also provided a way to measure the time it takes for a person to recognize an odor after it has been released into the air stream, and also the time it takes for a user to recognize that the odor is no longer present.

I would like to dedicate this thesis to my wife and children, whose love is invaluable.

CONTENTS

LIST OF TABLES

LIST OF FIGURES

ACKNOWLEDGMENTS

I would like to thank my wife Marti, without her love and support it wouldn't have been possible for me to be at this point in my life. I would also like to thank my parents for teaching me hard work, the importance of creativity and the importance of learning.

I would like to thank Mark Minor and John Hollerbach for the opportunity of working in the Robotic Systems Laboratory and with the TreadPort Active Wind Tunnel. And I would also like to thank Eric Pardyjak for sharing his expertise with me. Without his help the fluids work would not have been possible.

CHAPTER 1

INTRODUCTION

Virtual reality is becoming increasingly more important in today's life. Today's virtual environments can provide a means of therapy and rehabilitation [1-3], as well as job training. In traditional virtual environments the information being communicated tends to be only visual and auditory, which limits the effectiveness of the virtual reality as a means of communication. It has been shown by the authors of [4] that increasing the number of types of stimuli in the environment, for example, the addition of tactile and olfactory stimuli, increases the level of user presence in the simulation, making the virtual reality a more effective means of communication.

1.1 University of Utah TreadPort Virtual Environment

The University of Utah TreadPort Virtual Environment or UUTVE is a virtual environment that endeavors to help its user be as present in the virtual reality as possible, by including as many of the stimuli we experience in everyday life incorporated into the environment as possible. The UUTVE consists of; a CAVE like visual display [5], an auditory display, and locomotion interface [6, 7]. Recently a wind display has been added

to the UUTVE called the TreadPort Active Wind Tunnel or TPAWT. This display provides the tactile stimulus of the air as it flows around a person.

The TPAWT is a two-dimensional wind tunnel capable of generating air flow that "appears" to be coming out of the virtual environment [8]. Figure 1 shows a plan view of the inside of the TPAWT as well as the duct work. The wind is generated by pulling air into the fan through the back of the wind tunnel and pushing the air through the vents to the air inlets. The velocity of the wind at either inlet can be controlled using valves within the duct work. The development of the TPAWT is the subject of the work done by Kulkarni, Fisher, Desai and Chakravarthy [9-12].

To create the appearance that the air is coming from the screens, the air from the ducts is vented along the entire height of three 8x8 foot viewing screens that make up the visual display. One of these vents is shown in Figure 2. As the air streams move along the screens from different directions, the air streams meet. When they meet, the air is deflected away from the screens and out into the room towards where the user is standing. Thus the wind "appears" to be coming from the environment. By using the valves in the ducts to determine how fast or slow the air comes out of the air inlets relative to each other, the direction of the wind changes. After the air moves past the user, it is pull through a bank of filters and recirculated back into the ducts by the fan. The wind information displayed in the environment comes from wind simulations provided by the Quick Urban Industrial Complex or QUIC dispersion modeling system [13-15].

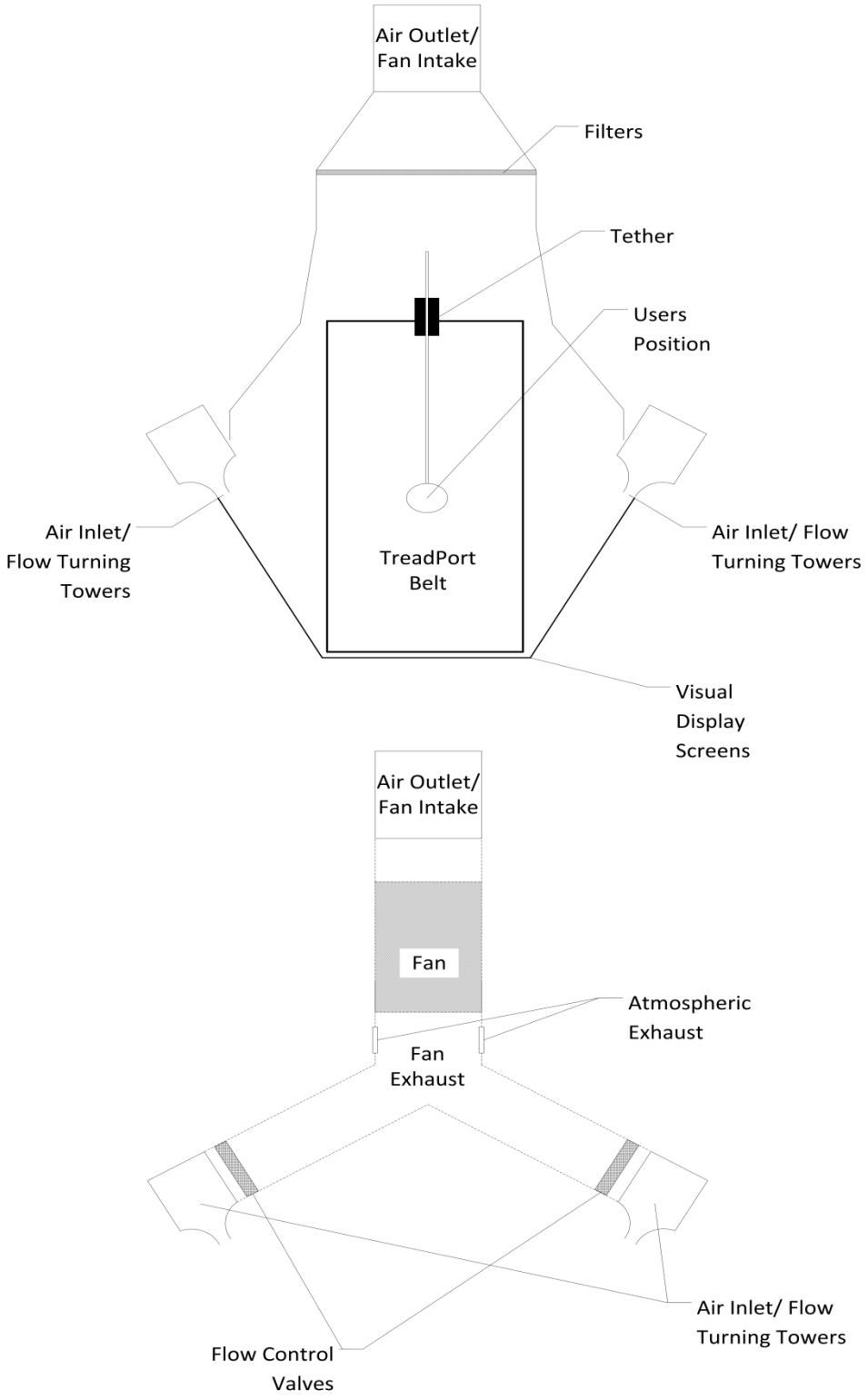

Figure 1. Diagram of the UUTVE/TPAWT showing the display screens, locomotion interface and wind generation components.

Figure 2. The vent out of which the air is blown along the screen.

1.2 Olfactory Display

In creating the olfactory display, a few questions need to be asked. How will the scent be delivered to the user? Where will the delivery system be put? How will the delivery system be controlled?

Because of the nature of the air flowing through the wind tunnel it is easy to infer that scent particles released upwind of the user will be carried to the user. What is not easy to infer is what state the particles will be in by the time they reach the user. Will they be so dilute that the user will not be able to detect the scent or perhaps will they be

clumped together and provide only a short strong burst of scent, or something in between? These questions lead to the idea of using Computational Fluid Dynamics (CFD) to model the air flow and dispersion of the scent particles, to get a feel for how the scent particles will behave.

Using a simplified 2D representation of the geometry of the wind tunnel the wind flow fields can be obtained, but before dispersion can be simulated, the release point of the scent must be known. This point is based on the placement of the scent injection system and this placement is based on the design of the scent injection system.

In designing the scent injectors an important function of the injector is that the scent be atomized as it is injected into the air stream. This atomization is important because it improves the efficiency of the scent delivery, and with this in mind, the first idea for releasing the scent into the air was to use an automotive fuel injector. This was an attractive idea because it encompassed an atomizing nozzle to spray the scent and a method for controlling the nozzle in one package. However, there were problems with using the fuel injector; first, we were not able to provide the pressures needed to get a nice atomization of the scent liquid, and second, the scent liquid was being put under pressure and putting the scent under pressure did not seem like a good idea as the scents being used might be flammable.

The second method that was explored, and ultimately selected as the desired method for getting the scent into the air, was to use an air atomizing siphon/gravity feed nozzle. This nozzle uses air flowing through the nozzle to the atmosphere to draw out the scent liquid and atomize the liquid as it is injected into the atmosphere. The control of the

air flow to the nozzle is achieved by a solenoid. This method proved effective at getting the scent into the air at air pressures much lower than were needed for the fuel injector.

The placement options of this injector design were limited by the concern that if the scent bottle was place above the nozzle a siphon effect would cause the scent to leak out of the nozzle and drip on to the ground and also the desire to keep the injectors out of the wind stream as much as possible. This removed placing the nozzle in the ceiling as an option, because to keep the nozzles presence at a minimum in the environment only the nozzle would be below the ceiling. Thus requiring the scent containers to be above the nozzle and increasing the likelihood of scent siphoning out of the bottle. Placing the injector at the floor was rejected as an option because of space issues with the locomotion interface.

This left the air inlets as the most reasonable place to put the nozzles because the nozzle could be placed in the air stream while keeping the scent bottle below the nozzle and out of the air stream as well. The final placement of the nozzle is shown in Figure 3 and Figure 4. Figure 3 shows the nozzle with the scent container mounted to the outside of the air inlet and Figure 4 shows the inside placement of the nozzle with a close up of the nozzle. Placing the nozzles at this point is not without its own downsides. For one, the air inlets are some distance from where the user stands and it would also require modifications to the air inlets, in the form of holes. Despite these drawbacks placing the nozzles in the air inlets provided the best option. This option also meant that there would need to be a nozzle in each of the air inlets to maintain symmetry.

With the placement of the injector chosen, the CFD model can be developed and the particle dispersions can be simulated. To get a sufficiently broad picture of the how

Figure 3. Nozzle and scent container mounted to the outside of the air inlets, with the scent lower than the nozzle.

Figure 4. Nozzles position as installed with a close up of the nozzle.

the scents disperse through the wind tunnel, simulations for different wind speeds and different lengths of time that scent is injected into the air stream are required. Once the simulations have been completed, the concentration data from the simulations can be used to create equations that describe how the concentration at the user's position behaves for different wind speeds and injection times.

Lastly experiments verifying the model developed from the simulations should be conducted. The quantities to be measured in the experiments include the time it takes for the scent particles to reach the user, called the delay time and the amount of time that the user senses an odor, called the residence time.

1.3 Related Work

The group lead by T. Nakamoto has been very active in the research and development of olfactory displays. They have developed a wearable olfactory display that can display up to 32 scents [16] and uses solenoids like our system. However, in their injection system there is a constant flow of air to the outlet of the device and when the solenoids, which are connected to scent jars, are activated, evaporated scent particles from the jars are drawn out the exit of the device and displayed to the user. To control the solenoids of their display they developed a delta-sigma modulation [17], which is like pulse width modulation. They have also improved their display by using rapid-switching solenoids [16]. In their research they used their display to include scents in a movie [18] and also computer game [19] and shown an increase in user presence with the inclusion of the display.

Sakamoto et al. have also developed a solenoid based table top display like that of Nakamoto's that does nose detection [20]. They have developed their display in conjunction with a visual display. The work they have focused on is that of reminiscence therapy and life review therapy where the scents are used to help trigger memories [21].

Using a technique similar to Nakamoto's group, T. Yamada et al. have created a wearable and portable display that was then used in localization of a scent source[22]. Their display uses an inkjet cartridge to inject the scent into the moving air sent to the user's nose. Scent localization is something that would be possible with the olfactory display developed for the TPAWT.

In the localization and display of scents in a virtual reality, work has been done by H. Matsukura to develop CFD models of how scent particles would disperse in a virtual reality simulation [23, 24]. This use of CFD is different from our use of CFD. We use CFD to model how the scent particles will travel in the wind tunnel not to find what the concentrations should be simulated to be at a given position. The simulations done by Matsukura are more along the line of the information that would be received from the QUIC software.

Other displays using inkjet cartridges have been developed to spray the scents directly in to the air. This kind of display typically sits a short distance away from the user and has the advantage of not requiring the user to wear anything. However scents persisting in the area around the user and the user becoming saturated to the smell can become an issue. The measurement of specific parameters like the delay time and residence time of the display are measured in [25] by A. Kadowaki et al. and in [26] by Sugimoto et al. The minimum time that is necessary between two pulses so that the

separate pulses can be distinguished is also found. This information is then used to develop methods of injecting the scents so that the air does not become overladen with scent or the subject does not become saturated with smell. This is the same type of work that we have done for our display in determining how well the CFD model works. Then in [27] by Kadowaki et al., a sensor to detect the breathing of the user is developed, allowing the release of scent to coincide with the inspiration of the user. The issue of the scent lingering is not a problem with the TPAWT because as the air flows around the user it is pulled away from the user. However, the user can become saturated with scent if too large a scent pulse is released at one time.

Sugimoto et al. have taken their device and applied it to the idea of incorporating olfactory stimulation into advertising [28]. Their olfactory display is mobile and as a person walks toward or away from a given advertisement sign the concentration of odor is respectively increased and then decreased. This is very similar to the odor localization discussed previously.

The olfactory display that has been developed by Y. Yanagida et al. is able to project scent over moderate distances [29]. This display uses an air cannon to create a toroidal vortice that travels through the air. By using nose tracking software, the scent is shot at the user's nose. The disadvantage to this display is that it requires more than one cannon. However an advantage is that it does not require the user to wear the display as they move about the environments space. This is similar to our display in that the user doesn't have to wear anything. However, our system has the advantage of the locomotion interface which means that as the person moves about the virtual reality they do not move

in any significant manner in the physical world and the scents can be sent over a distance and tracking of the user is not necessary.

An issue that can arise with some displays is that of noise being generated. This is especially true of the displays that use solenoids. So in [30], D. W. Kim et al. have developed a display that uses temperature sensitive scent gels. When the gels are heated the desired scent is produced and the issue of sound being generated is no longer a problem.

Another issue that arises in making olfactory displays is that of scents with low volatility. When scents have low volatility they have a hard time keeping up with the need of the display because the scent cannot evaporate fast enough. Some methods have been developed and used with success to remedy this problem. In [31] Nakamoto et al. have developed an inkjet cartridge display that sprays the scent particles on to a mesh heater, which forcefully evaporates the scent particles. Building on this idea Y. Ariyakul et al. use an electro osmotic pump and surface acoustic wave device to get the scent particles to atomize [32].

One of the greatest issues in creating an olfactory display is how to present all the odors that might be experienced in the course of life. So far a set of “primary odors” that can be used to create any desired odor have not been found. There are some different ways to overcome this; one, is to make an olfactory display where the constituent odors of the display have been chosen, as described by T. Nakamoto et al., so that the desired odor is approximated by superimposing the constituent odors of the display together [33]. Another way developed by Nambu et al. found in [34], uses the cross modality of

olfaction and vision. Where vision informs the smelling process, this phenomenon is discussed by Gottfried et al. in [35].

1.4 Contributions

The development of an olfactory display for the UUTVE helps the UUTVE become an even more versatile virtual environment by enabling the UUTVE to be used in experiments to determine the effects of olfaction on rehabilitation and training. By using CFD to create a model of the particle dispersion a method for the future control of the olfactory display is developed and a greater understanding of the air flow physics in the wind tunnel is obtained. The experiments that are done help in the validation process of the CFD model and also tell us that the olfactory display works at presenting scents to a user of the UUTVE.

1.5 Thesis Outline

The rest of this thesis details the development of the olfactory display for the UUTVE. The first topic discussed is the physical setup of the olfactory display and is found in Chapter 2. Then in Chapter 3 the development of fluid simulations used to model the particle dispersion in the TPAWT is discussed. Chapter 4 presents the experimental results, with the smoke visualization experiments given in 4.1 and the results of the user studies given in section 4.2. Finally in Chapter 5 a discussion of the project is given.

CHAPTER 2

OLFACTORY DISPLAY

The olfactory display is made up of a few different components; the nozzles and solenoids, the air delivery system, and the scents and their containers. The nozzles and solenoids and the control of the solenoids is discussed in section 2.1. The air delivery system is discussed in section 2.2. Section 2.3 discusses the scents and the scents containers.

2.1 The Nozzles and Solenoids

To get the scent particles into the air stream, an air atomizing nozzle from the Spraying Systems Co. was chosen, (part number 1/8J+SUF1). This nozzle uses compressed air to siphon the scent particles from the container and then eject the particles out of the nozzle. The nozzle has a tip that produces a fan spray pattern, described in Figure 5 and Table 1 for different operating pressures, this information comes from the Spraying Systems Co.'s catalog [36]. The nozzle is oriented so that the flat plane of the spray is parallel to the screens and sprays at an angle into the air stream. Figure 6 shows a view of the nozzle and solenoid together from the outside of the TPAWT. The solenoid attaches to the outside wall of the air inlet.

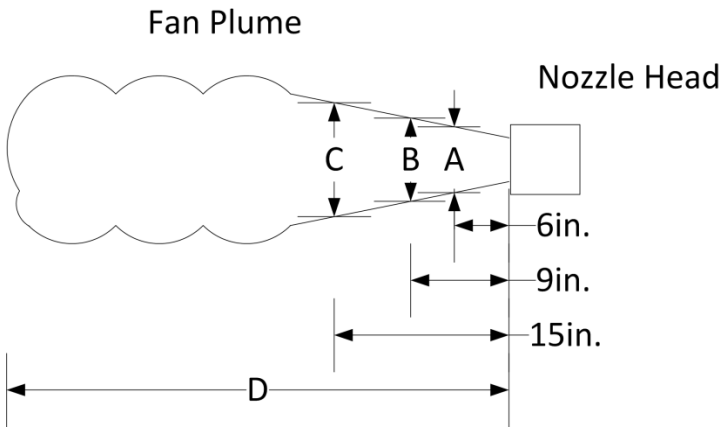

Figure 5. Nozzle fan dimensions, flow is from left to right.

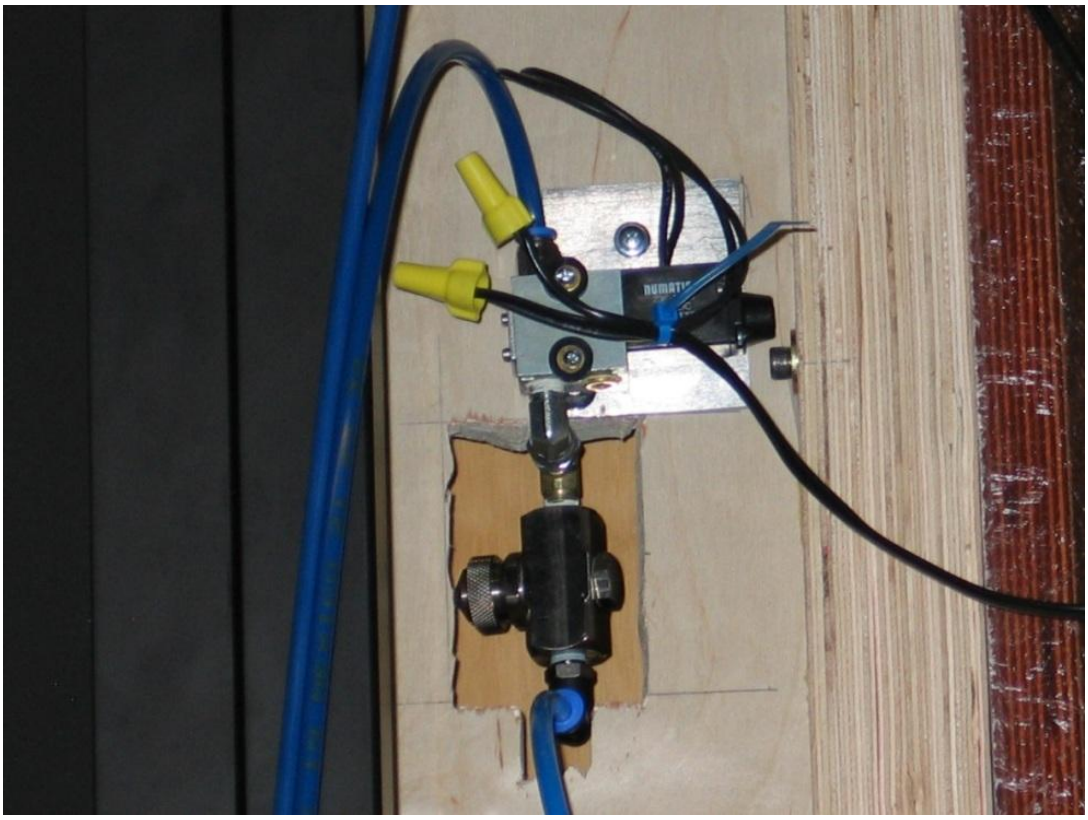

Figure 6. Nozzle with solenoid.

Table 1. Nozzle spray dimensions for different operating pressures.

Air Pressure (psi)	A (in)	B (in)	C (in)	D (ft)
10	8	10.5	15	7
20	8.5	11.5	15	7
30	9	12	15	6

The air to the nozzle that creates the siphon action is controlled by a Numatics 12V DC solenoid, (part number L01SA459O000060). Direct control of the solenoids using the dSPACE DS1103 PPC Controller Board was not possible, so an intermediary circuit was needed and is shown in Figure 7. The DS1103 is programmed using Matlab and Simulink.

At first, when the solenoids would actuate, the vibrations caused by the actuation would be amplified by the wall of the air inlets. This sound was loud enough that it would distract a user from the environment. So to remove this distraction the solenoid and nozzle assemblies were isolated from the wall of the air inlet by using rubber washers, while the sound was not completely removed the sound that was emitted was reduced to levels that would not distract the user from the environment.

2.2 Air Delivery System

To provide the compressed air to the solenoid and nozzle, a ten gallon air tank shown in Figure 8 was used because there is no dedicated pressure airline in the TreadPort lab. The tank is filled to 100 psi then regulated twice, once to 40 psi, then again to 25 psi. The air is regulated twice so that the air pressure at the nozzle is as

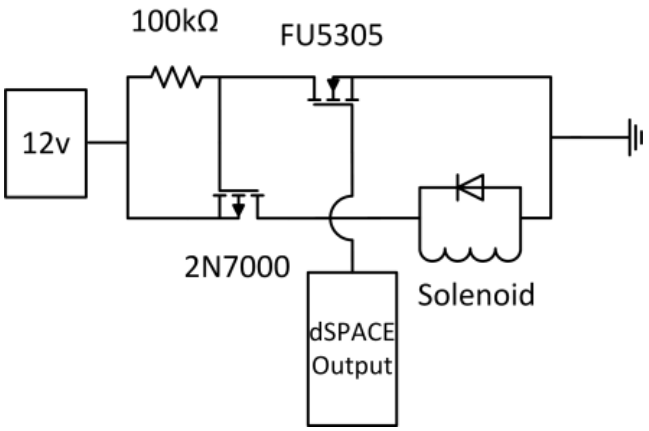

Figure 7. Solenoid control circut.

Figure 8. Ten gallon air tank.

constant as possible as the pressure in the tank decreases. When the final pressure is regulated to 25 psi there is enough air for about 10 minutes of continuous air flow or four to five user experiments that last about 5 minutes apiece. Figure 9 shows a schematic of the air flow through the delivery system. The compress air flows from the air tank through the regulators. Then from the regulators the air is split between the two solenoids. From the solenoids the air goes into the nozzles and flows out. As the compressed air flows out of the nozzles, air from the atmosphere is drawn through the scent containers to the nozzles and the scent particles are ejected out in to the air stream.

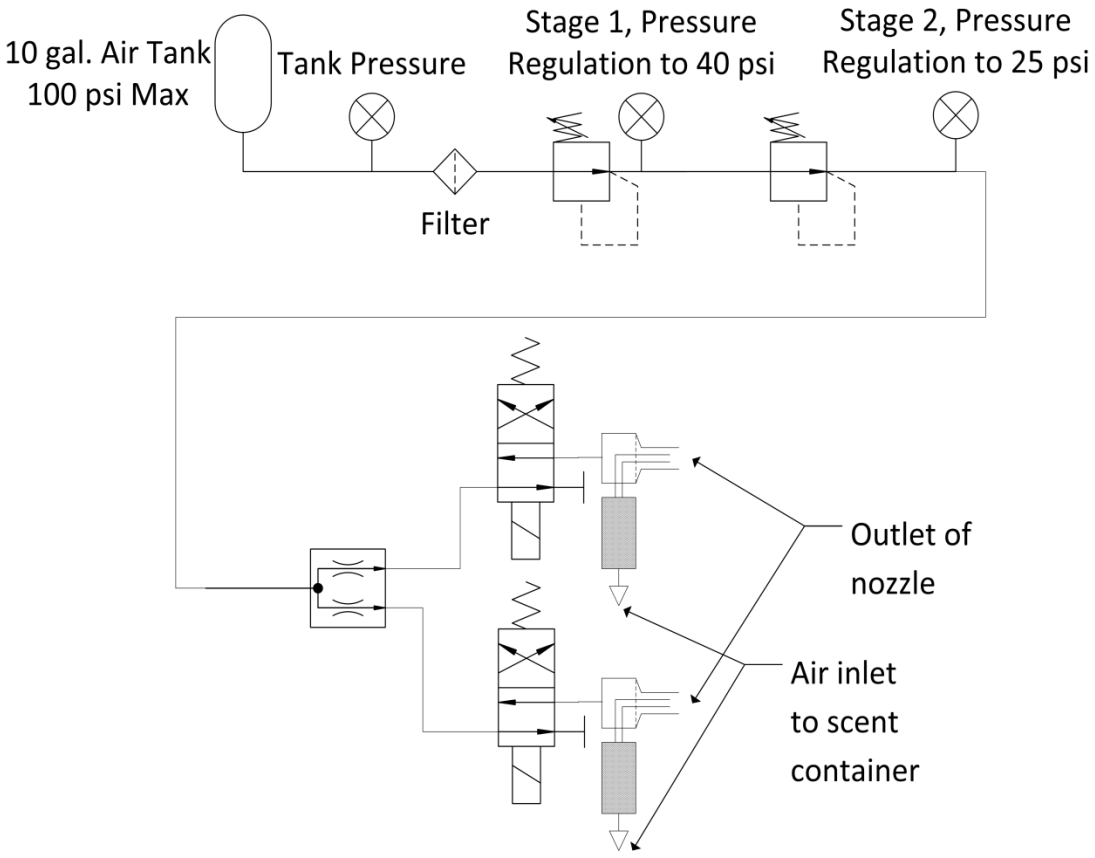

Figure 9. Schematic of the injection system.

When the solenoids are activated and the air escapes out of the nozzles a hissing noise is produced. Like the noise from the solenoids actuating, this noise is also distracting. By reducing the pressure at the nozzle the level of noise was reduced, however the pressure could not be reduced too much or there was not enough air flow to get the proper suction through the scent containers.

2.3 Scents and Scent Containers

In creating the first scent container prototype it was thought that the scent oil could be sprayed directly out of the container, but doing this caused too much scent to be sprayed out and the TPAWT would become totally saturated with the smell. The next prototype used a cotton ball saturated with the scent oil and as the solenoids actuated and pulled the air through the scent container the air is pulled through the cotton ball and the scent oil was pulled along with the air. This design greatly improved the performance of the display, but the scents were still too strong. To further reduce the amount of scent being injected, the scent oil was mixed, half and half with extra virgin olive oil. The olive oil had a very mild almost imperceptible smell that did not interfere with the smell of the scent oil. Figure 10 shows the container with the hose that connects to the nozzle. Figure 11 shows the container with the inlet hole and Figure 12 shows the inside of the container with and without the cotton ball.

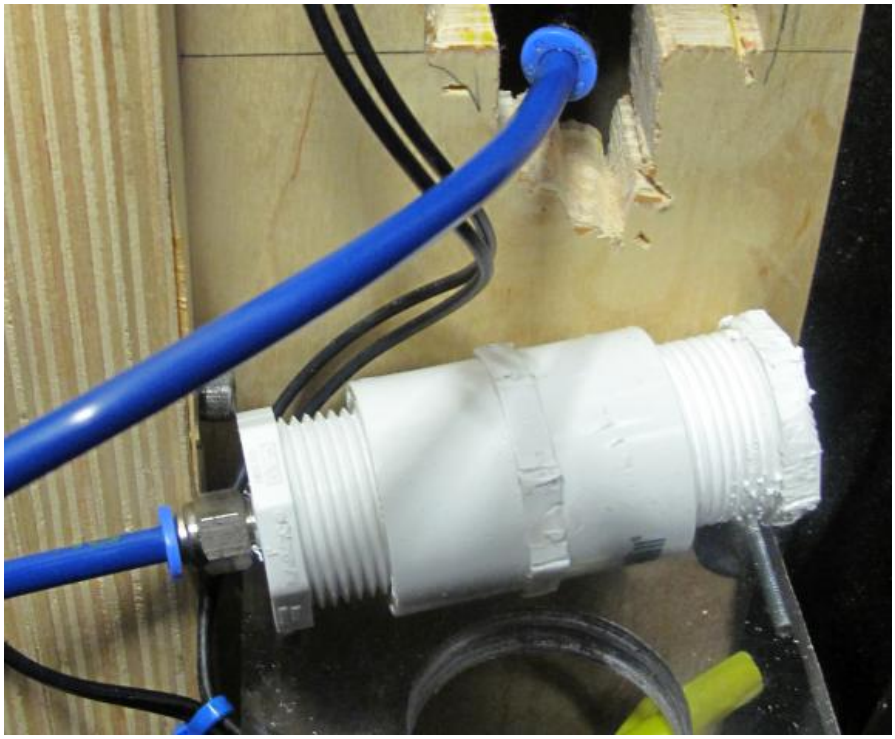

Figure 10. Scent container.

Figure 11. Scent container from a different angle, showing air inlet hole.

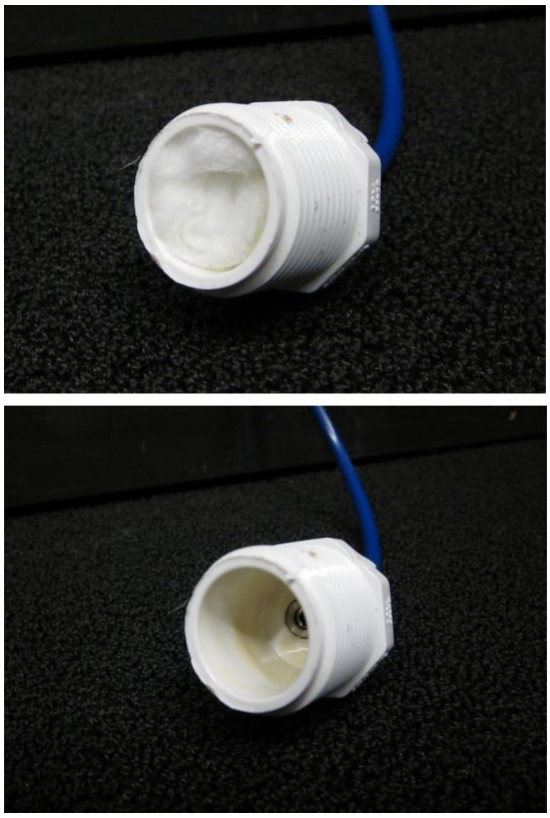

Figure 12. Inside of container, the top has the saturated cotton ball shown, bottom does not have the cotton ball shown.

CHAPTER 3

FLUENT SIMULATIONS

To determine if the wind generation capabilities of the TPAWT could carry the scent particles to a person using the UUTVE, CFD particle dispersion simulations were conducted in Fluent version 6.2 [37]. These simulations have two purposes: to evaluate how particles would flow through the environment and to determine how the concentration of the particles at the user's position would change over time for different wind speeds and for different particle release times known as injection times. With this information we can create a model that can be used to predict the concentration behavior of the system for these different wind speeds and different injection times.

The simulations were done for six wind speeds at the air inlets: 2, 3, 4, 5, 6, and 7 meters per second, and for five different injection times: 0.5, 1, 1.5, 2, and 3 seconds.

In section 3.1 the setup of the simulations is given then in section 3.2 the results of the simulations are presented. Section 3.3 discusses the nondimensionalization of the data from section 3.2 and the creation of a model that describes the systems behavior. Section 3.4 discusses how well the simulation data matches the model and lastly section 3.5 relays the conclusions of the simulation work.

3.1 Simulation Setup

For the simulation, a simplified 2D model of the TPAWT geometry and finite volume mesh was created in Gambit using the same configuration used by Kulkarni in the development of the wind tunnel [12]. The geometry and mesh was then used in Fluent to create the CFD model of the air flow. The simulation uses an unsteady time solver, and the k-ε model [38] for turbulence, and stochastic tracking and a discrete random walk model for the unsteady particles. The simulation also uses the default settings for a pressure based solution and the turbulent kinetic energy in the Fluent environment. For each of the different wind speeds the simulation was iterated until the flow field inside of the room was resolved. Figure 13 shows the flow field for an air velocity of 3m/s at the inlets. After the flow field was resolved for the different velocities, the particles representing the scent were injected for 0.5, 1, 1.5, 2, and 3 seconds into the room from the air inlet surfaces.

The scent's density and mass flow rate, as well as the velocity of the scent out of the vents, are needed for the simulations of the injection. The density was measured by weighing a known volume of scent oil and the mass flow rate was measured by weighing the scent bottles before and after a given amount of time of the injectors spraying. With these measurements and the measurements of the nozzle outlet the scent particle velocity was calculated. The properties measured and calculated are found in Table 2.

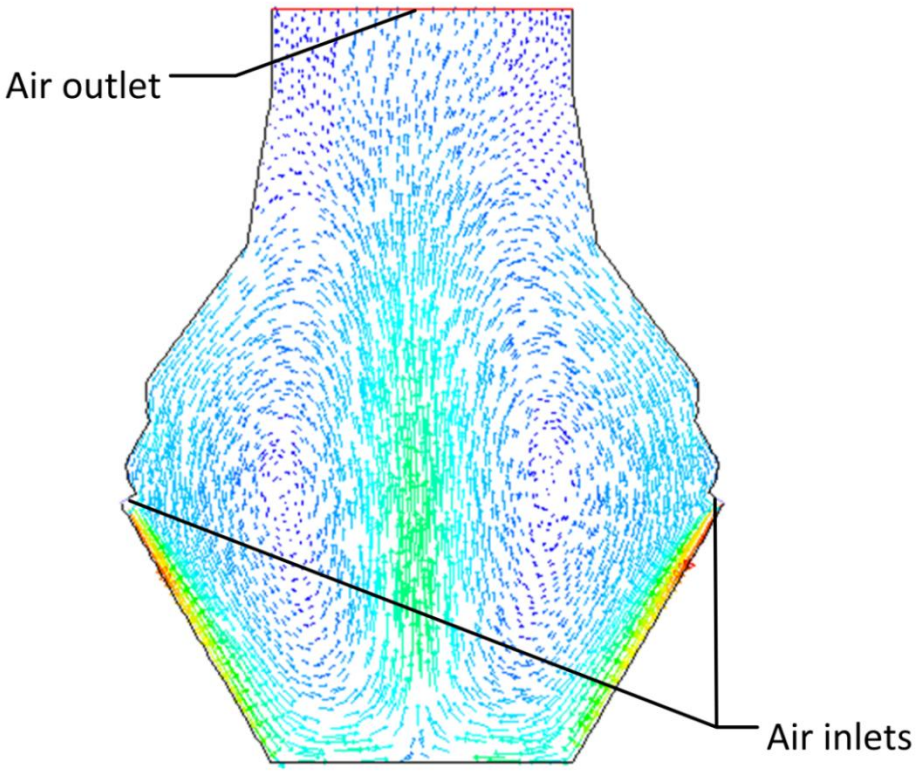

Figure 13. Velocity vectors for 3m/s vent exit wind speed. The red arrows represent wind air traveling at 3m/s, the dark blue represents slow moving air.

Table 2. Important Injection experiment parameters

Liquid Scent Density (kg/m^3)	987.5
Mass flow rate (kg/s)	1.6x10^{-5}
Particle flow rate (particles/s)	1.2962x10^14
Particle velocity (m/s)	0.018
Nozzle width (m)	0.5x10^{-3}
Nozzle length (m)	1.8x10^{-3}
Particle diameter (m)	1x10^{-7}

3.2 Simulation Results

As one of the purposes of the simulations was to determine if the scent particles would reach the user, snap shots of the particles flowing through the system were taken. This was only done for the case of a 1.5 m/s inlet wind speed and 0.5 second injection time. Figure 14 shows these snap shots. In it we see the progression of the particles as they move along the screen, then towards the user's position represented by the black line. After the particles pass by the user's position we see that most of the particles travel towards the air outlet and leave the system: however, some of the particles get trapped in the vortices seen in Figure 14 and recirculate back toward the user's position. This tells us that according to the simulations, if the scent injectors are place at the air inlets the scent particles will reach the user.

The other purpose of the simulations was to determine how the concentration at the user's position would behave with time as a function of the wind velocity and the injection time. Figure 15 shows the concentration curves versus time for the different injection times (0.5, 1, 1.5, 2, and 3 seconds) and at different wind velocities (2, 3, 4, 5, 6, and 7 m/s).

In this figure, we see that as the injection time increases the amount of time that the concentration stays in the system increases; however as the wind speed increases we see that the concentration levels decrease and that it does not take as long for the scent particles to reach the users position. We also see that as the wind speed increases the concentration starts to plateau for longer injection times. Also, with the increase in wind speed, there is a decrease in the amount of time that the main group of particles spends at the user's position. After the main group of particles pass the user's position there is

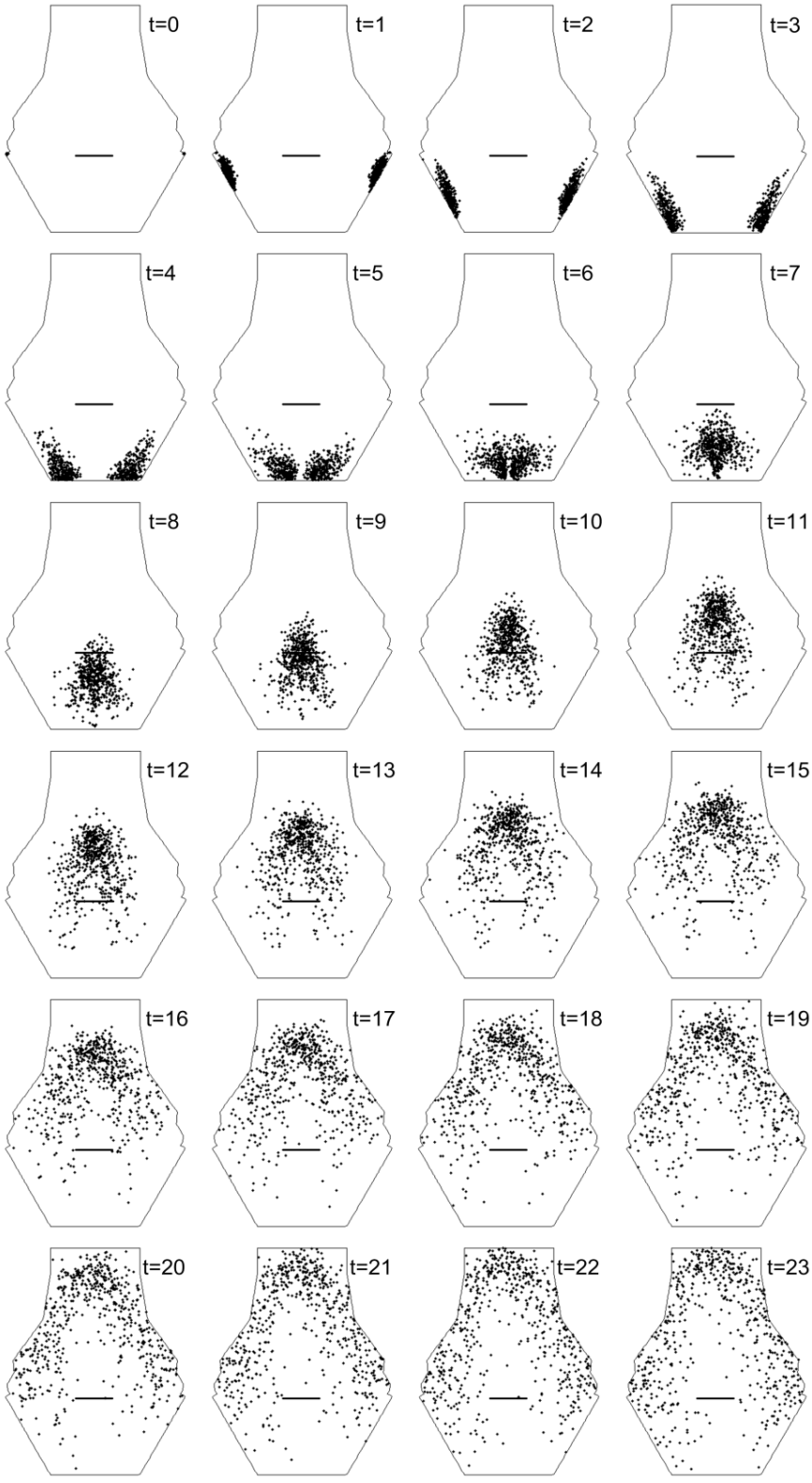

Figure 14. Simulation of particle dispersion, time is in seconds.

another small rise in the concentration, which then slowly decreases with time. This rise is associated with the particles that get trapped in the vortices and recirculate back to the user's position.

The relationship of velocity at the air inlets to the velocity simulated at the user is given in Table 3. The mean and max velocities are taken from the black line that represents where the user position is, as seen in Figure 14. The effective velocity is calculated by dividing the distance that the particles travel by the time it takes for the particles to travel that distance for each of the different inlet wind speeds.

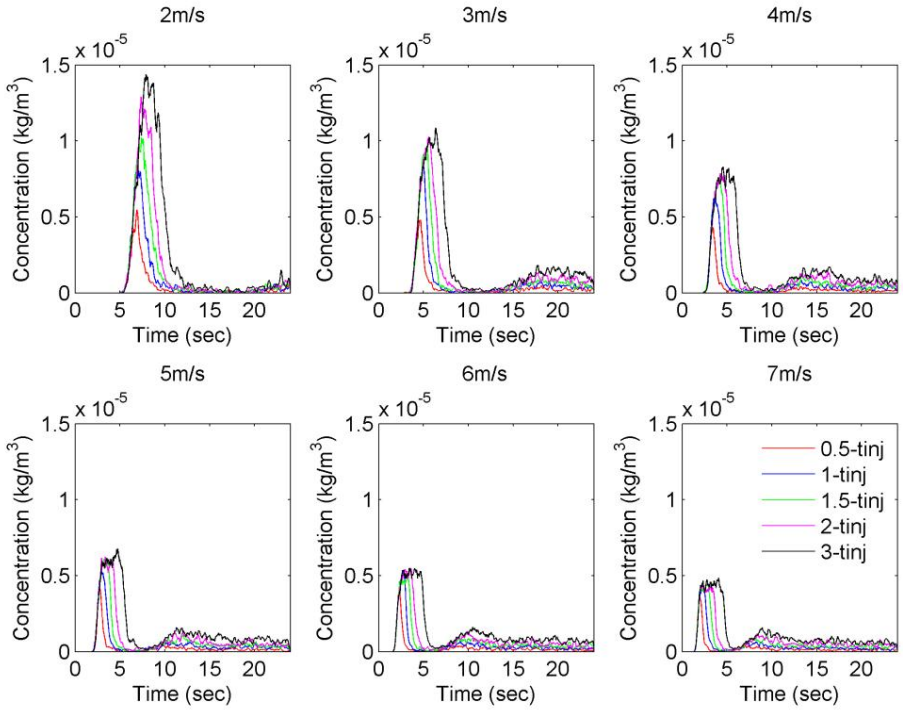

Figure 15. Filtered data from simulations each frame shows the different wind velocities. The colored lines represent different injection times; red is 0.5 seconds, blue is 1 second, green is 1.5 seconds, magenta is 2 seconds, and black for 3 seconds.

Table 3. Velocity at the inlets with associated mean, max, and effective velocity at the user.

	User velocity (m/s)		
Inlet velocity (m/s)	mean	max	effective
2	0.67	0.88	1.03
3	0.99	1.32	1.64
4	1.32	1.78	2.20
5	1.66	2.24	2.73
6	1.98	2.70	3.34
7	2.31	3.16	4.07

3.3 Results Analysis

The analysis of the results is broken into two parts: the nondimensionalization of the simulation data, section 3.3.1, and the creation of a model from the nondimensionalization, section 3.3.2.

3.3.1 Nondimensionalization

To create a model of the concentration behavior shown in Figure 15 it is convenient to transform the data. This transformation is created by nondimensionalizing the concentration and time for each of the different simulations, these nondimensionalizations are a way of normalizing data. The goal of the nondimensionalization is to bring the concentration curves into one generalized curve that can then be modeled. The nondimensional equations were developed using Buckingham-Pi analysis [39]. This analysis gave the following nondimensionalization for concentration,

$$C^* = \frac{C v_{eff} l^2}{Q},$$

and for time,

$$t_1{}^* = \frac{v_{eff} t}{s}.$$

where C is the concentration from the simulation, Q is the mass flow rate of particles into the system, l is a characteristic length associated with the users position and is equal to 1 meter, s is the distance associated with how far the particles travel before they reach the users position and is equal to 5.26 meters, v_{eff} is the effective velocity and, t is the time elapsed.

These nondimensionalizations were not able to collapse all of the concentration curves into one curve but, they were able to show general trends in the way the system behaved. They also helped in developing a new nondimensional equation that was able to collapse the data farther but still not perfectly. This new equation is given as,

$$C^* = \frac{C v_{eff} l^2}{Q} \left(\frac{v_{eff} t_{inj}}{s} \right)^{-0.2}$$

t_{inj} is the amount of time the particles are allowed into the system and the exponent of -0.2 was chosen by trial and error, where the new term comes from the dependence of C^* on the injection time.

The results of this new nondimensionalization for the wind speeds of; 2, 3, 4, 5, 6, and 7 m/s are given respectively in Figure 16(a-f). With the different injection times labeled. These figures show that for a given wind speed the injection time affects the magnitude of $C^*$and how long it takes for C^* to start decaying. We also see the second rise in $C^*$and its gradual decrease.

This nondimensional equation is a better representation of the systems physics because it includes the amount of time that particles are allowed into the system. This is an important factor because the concentration at the user's position is greatly influenced by the injection time as was seen in Figure 15.

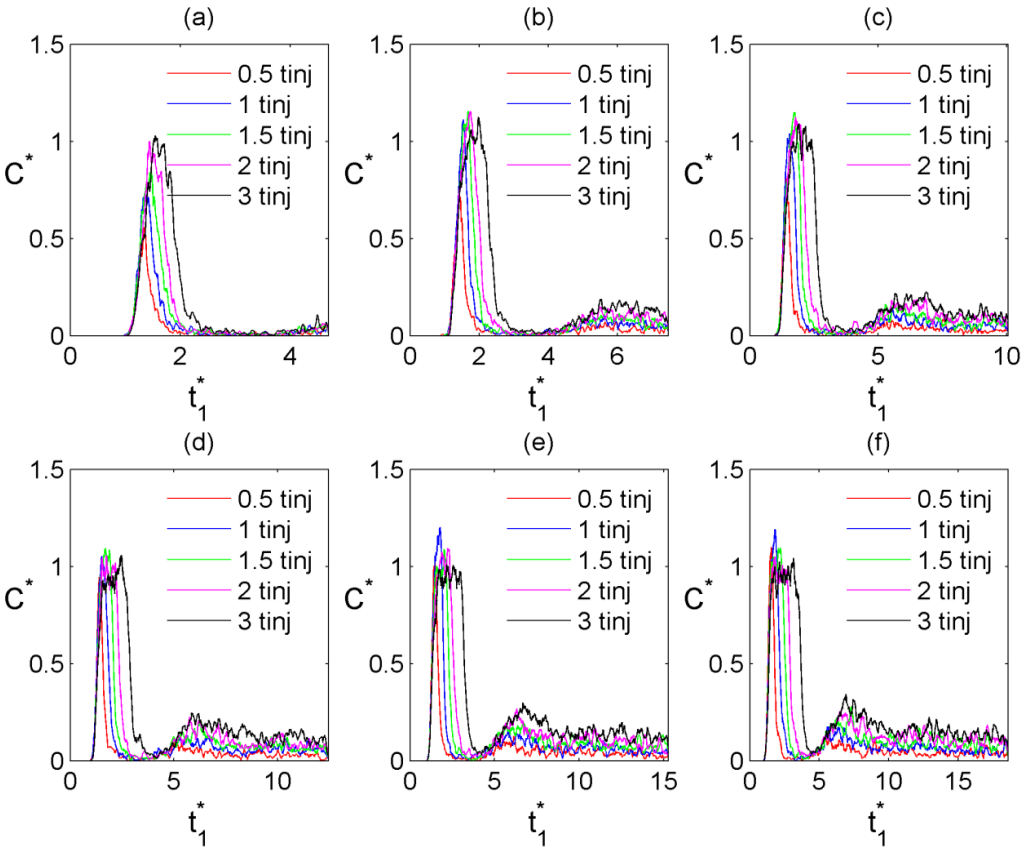

Figure 16. Nondimensionalized data for a wind speed; (a) 2m/s, (b) 3m/s, (c) 4m/s, (d) 5m/s, (e) 6m/s and (f) 7m/s.

By lumping all the C^*curves together and only focusing on the initial increase and decrease of C^*we obtain Figure 17. In this figure we see that for all of the cases of C^*, C^* begins to rise in the same place and depending on wind speed and injection time, C^*will increase and then at some time start decreasing or C^* will increase, plateau for some length of time, and then start to decrease.

The time at which C^* starts decreasing is important because it signals a change in the systems behavior and understanding this new behavior tells us how C^* decays. It is

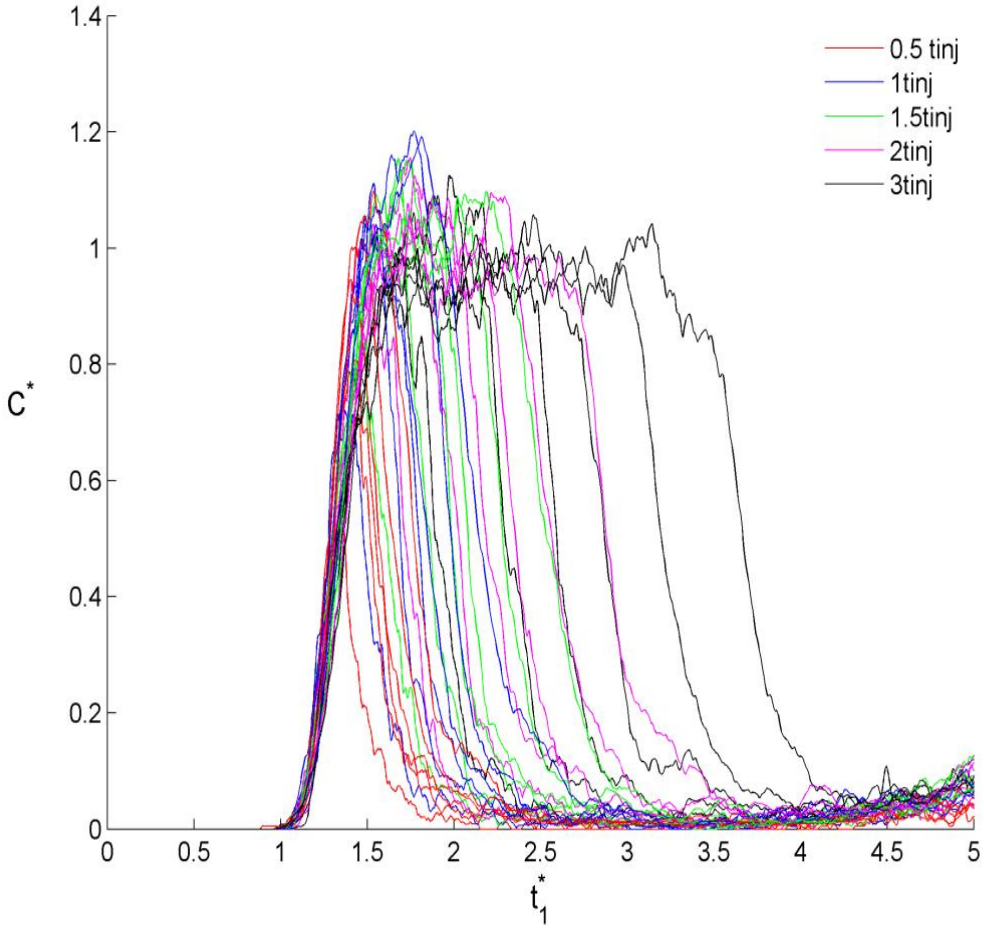

Figure 17. All of the nondimensionalized data lumped together.

also important to know if C^* decays in the same way for each case as well. To show that C^* does decay the same way in each case, a new nondimensional equation for t^* in which t_{inj} is subtracted from t is created. This equation is given below,

$$t_2{}^* = \frac{v_{eff}(t - t_{inj})}{s}.$$

This nondimensional equation gives the result shown in Figure 18, where the different colored lines again represent the injection time. In this figure we see that by subtracting t_{inj} from t the decaying curves together all line up together. Now that this nondimensionalization collapses the decaying portion of the C^* curves into one general curve, the decay can be modeled by a single best fit curve that represents how C^* decays for different injection times and wind speeds.

3.3.2 Model Development

The desired behavior that we want to model is that of $C^*$and t_1^*, shown in Figure 17. Because of the change in the behavior of the system there will be two pieces to the model. The first piece comes from modeling the rising and plateauing of C^*, which comes from the first nondimensionalization and the second part comes from modeling the decay of C^*, which comes from the second nondimensionalization, Figure 18.

Before the two parts can be modeled a t^* must be found that determines where the model transitions from one part to the other. This point is called t_{trans}^* and is calculated by finding the last t^* of C^* that is greater or equal to 80% of the maximum C^*

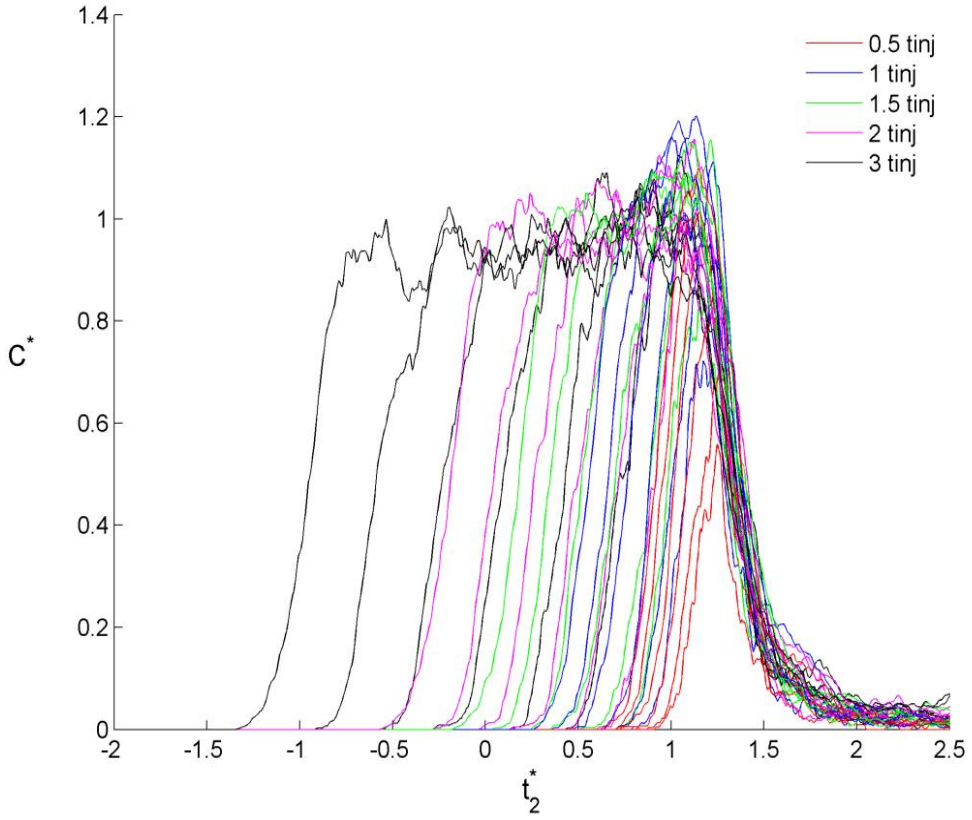

Figure 18. Second nondimensionalization for time.

for a given simulation. Figure 19 shows these points marked for each of the simulations. Now with t^*_{trans} known the nondimensionalization can be broken up into its respective behaviors. In section 3.3.2.1 the models for C^*increasing, plateauing and decaying are developed. Lastly a model of t^*_{trans}'s dependence on wind speed and injection time will be developed in section 3.3.2.2.

3.3.2.1 Rising and Falling Edge Models

Physically speaking there is no set of equations that describe how the concentration should behave. So it is necessary to find equations that fit the data the best

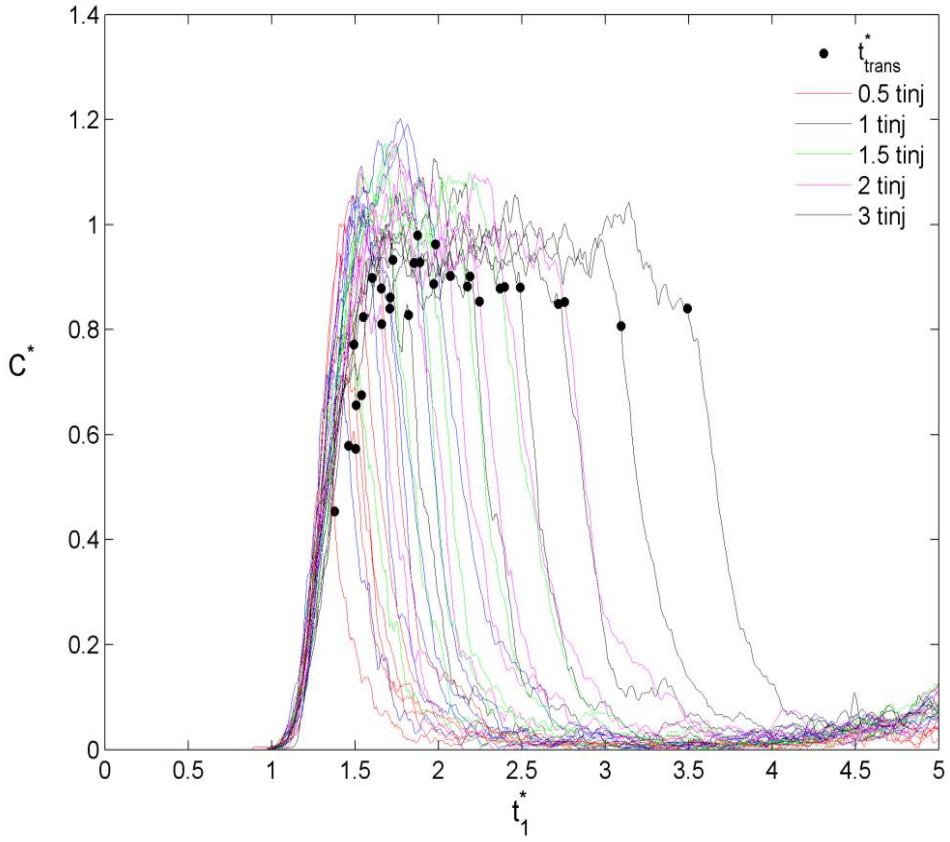

Figure 19. Nondimensional data with $\boldsymbol{t^*_{trans}}$ marked.

way possible. For the rising edge, a complimentary error function (erfc) was chosen. The data fit to the erfc is shown in Figure 20(a). To fit the erfc to the data the Matlab function lsqcurvefit was used. This function uses a least squares method to solve for the best fit. The resulting equation is,

$$C^*_{mr} = 0.5erfc(5.3474t^*_1 + 7.0633).$$

This equation is then plotted with the nondimensional data of C^* and t^*_1 in Figure 20(b). For the falling edge the system behavior to model comes from $C^*$and t^*_2 and is shown in

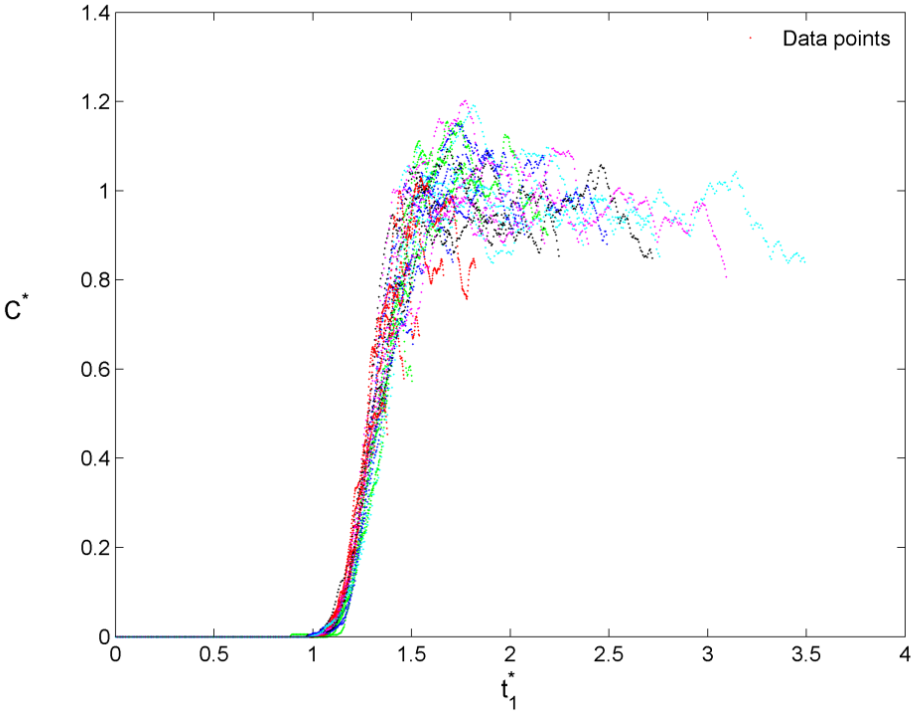

(a)

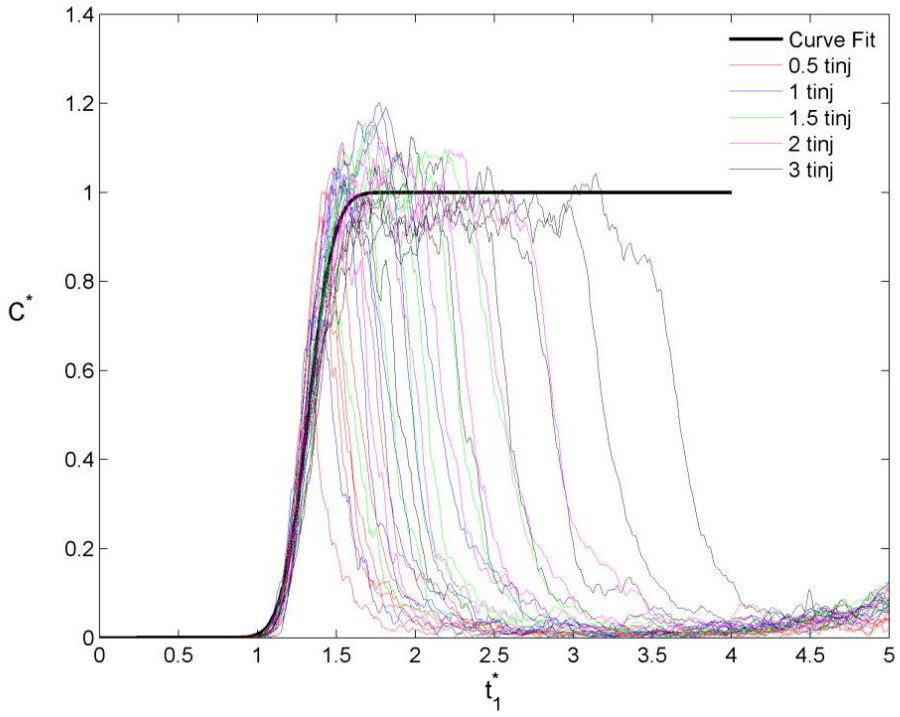

(b)

Figure 20. The nondimensional data to be fit is shown in (a) and the nondimensional data with curve fit plotted is shown in (b).

Figure 21(a). The model for C^* decay comes from the lumped data because fitting a curve all these points makes the fit more robust. When modeling the decay of concentration plumes, it is common for the decay behavior to decrease exponentially. This behavior is evidenced by a linear region when the data is plotted on a log-log scale. A log-log plot of the data has been generated and is shown in Figure 21(b), with the linear region marked. Again by using least squares curve fit this time fitting an exponentially decreasing function to the linear part in the log-log plot of the data, the equation below is obtained,

$$C^*_{mf} = 5.0354\mathrm{t}_2^{*\,-8.265}.$$

This equation is then plotted with that data points for $C^*$and t_2^* in Figure 22. This equation cannot be directly used to model the desired decaying behavior shown in Figure 17 because the concentration starts to decay in different places.

Thus there must be a transformation of t_2^* in C^*_{mf} to shift the curve so that depending on t^*_{trans}, C^* will decay in the desired place. This new t_2^* is found by solving C^*_{mf} for t_2^* when $C^*_{mf} = 1$ and then adding this value to t^* then subtracting t^*_{trans}. The new equation for t_2^* is given below,

$$t_2^* = t^* + \left(\frac{1}{5.0354}\right)^{\frac{-1}{8.265}} - t^*_{trans}.$$

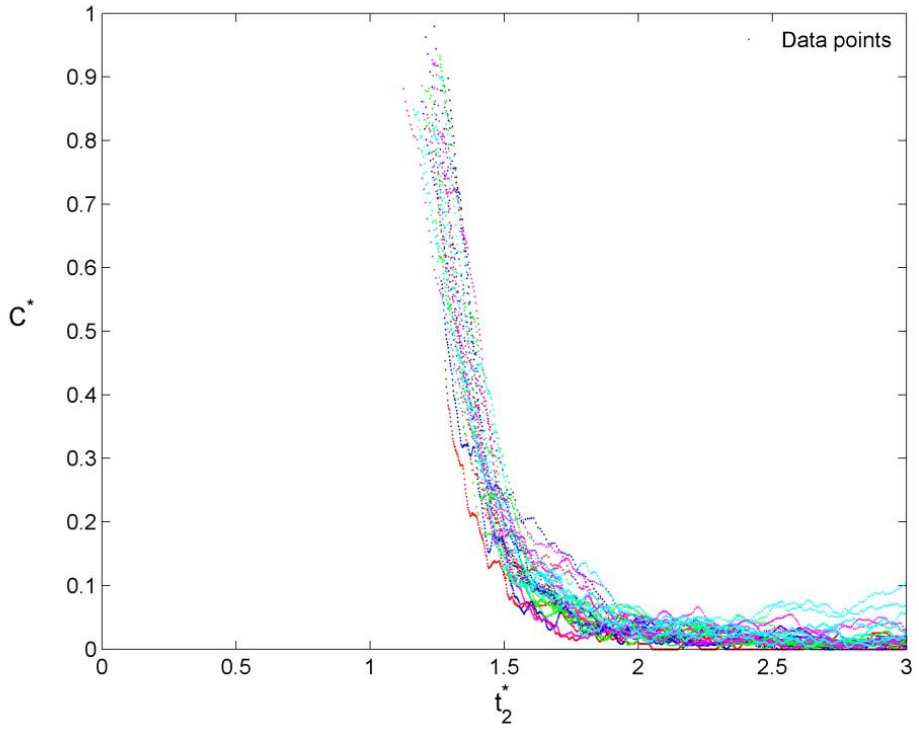

(a)

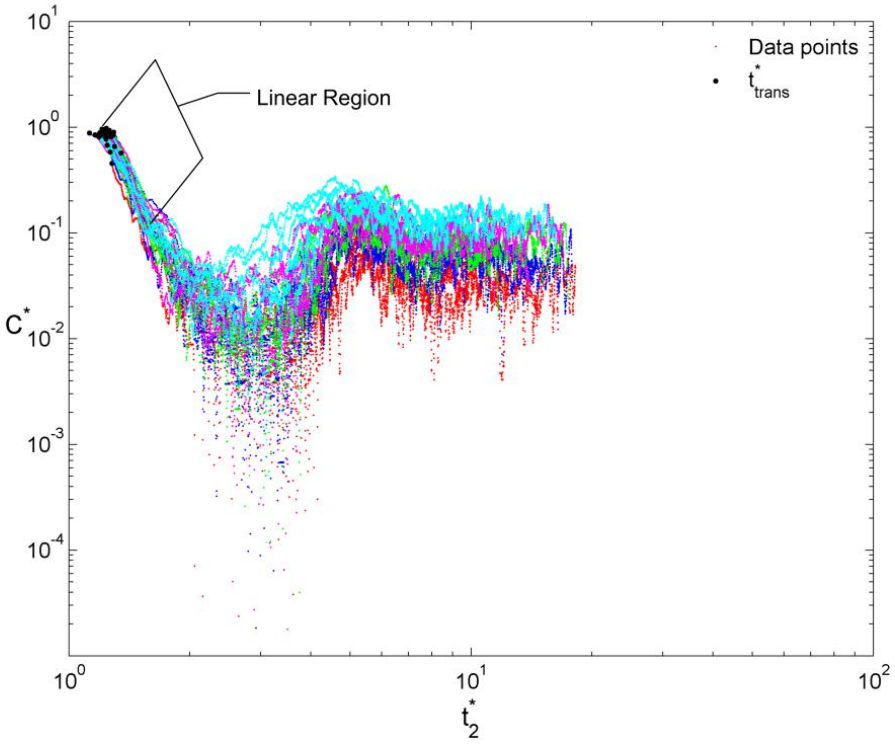

(b)

Figure 21. The falling edge nondimensional data to be fit is shown in (a) and the linear region on log-log plot is shown in (b).

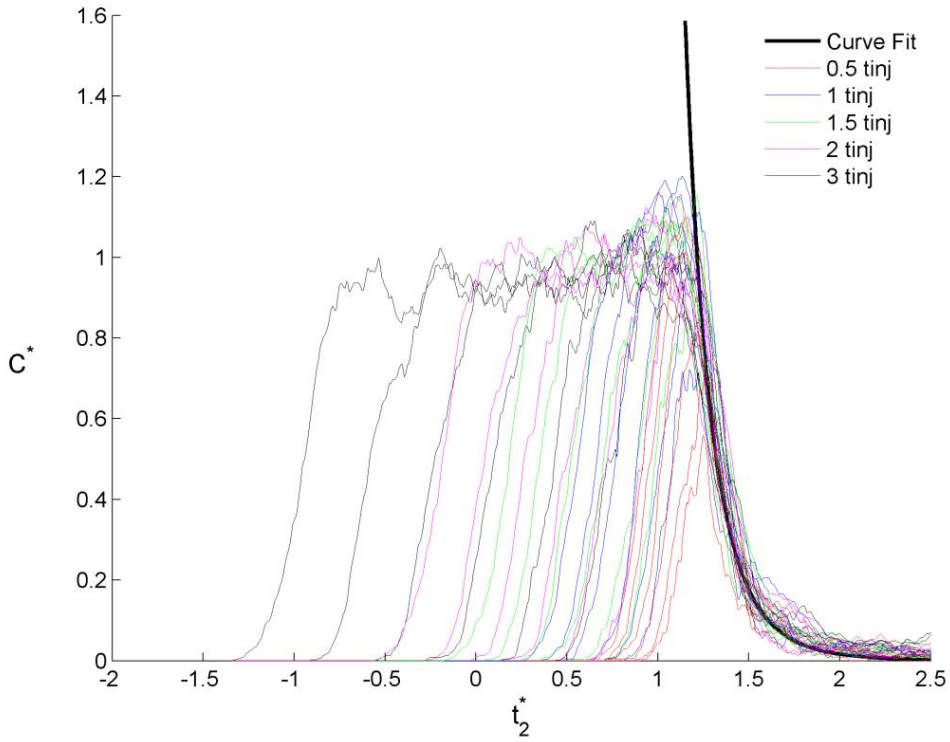

Figure 22. Nondimensionlizaion of $\boldsymbol{C^*}$and $\boldsymbol{t_2^*}$ with curve fit applied.

Thus the entire piecewise model becomes,

$$C_m^* = \begin{cases} 0.5erfc(5.3474t^* + 7.0633) & \text{for } t^* < t_{trans}^* \\ 5.0354\left(t^* + \left(\frac{1}{5.0354}\right)^{\frac{-1}{8.265}} - t_{trans}^*\right)^{-8.265} & \text{for } t^* > t_{trans}^* \end{cases}$$

Now all that is required is a way of determining what t_{trans}^* should be for a given wind speed and injection time.

3.3.2.2 Model of Transition Point

As has been stated the last part needed for the model is the relationship between t^*_{trans} and wind speed at the air inlets and the injection time. To develop this relationship, t^*_{trans} for each simulation was plotted with the associated wind speed and injection time and is given in Figure 23 as the red dots. Looking at the points alone it could be seen that a surface would fit these points. So using least squares regression a surface of the form,

$$s = ax + by + cxy + dx^2 + ey^2$$

was fit the transition point data. This fit is represented by the smooth surface in Figure 23

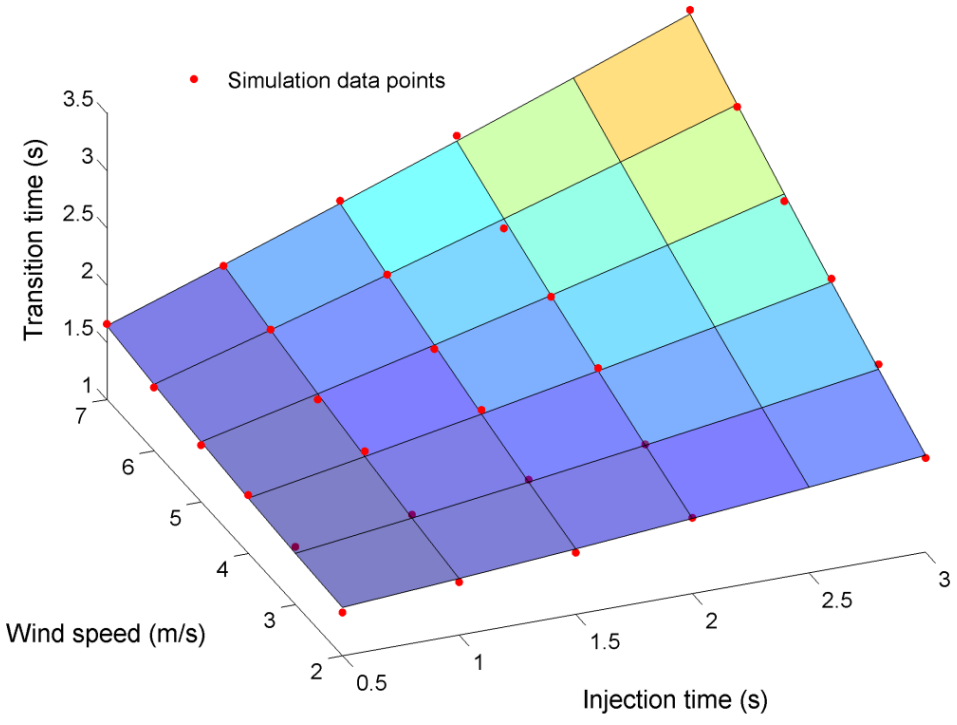

Figure 23. Transition points and the surface fit to these points.

and the equation for this surface is given below,

$$t^*_{trans} = 1.45t_{inj} - 0.1014v_{exit} - 0.0566t_{inj}v_{exit} + 0.1114{t_{inj}}^2 + 0.005{v_{exit}}^2.$$

With the piecewise model and the model for the transition point, a model of the overall system has been created where the nondimensional behavior of the system can be predicted given a wind speed and injection time. Then the inverse of the nondimensional equations can be applied to this model to give a model of what the concentration behavior of the system should be.

3.4 Model Verification

With the model developed, how well it performs needs to be established. To do this, standard error and fractional bias are used. Standard error [40] is a measure of the spread of the data around the fit curve and is calculated by the equation,

$$s_{y/x} = \sqrt{\frac{S_r}{n}},$$

where n is the number of data points and S_r is square of the residuals given by the equation,

$$S_r = \sum_{i=1}^{n} \left(C^*{}_i - C^*_{m_i}\right)^2$$

The results for the standard error are given in Table 4, in it, it can be seen that the standard errors are all small, suggesting that the model does a good job of predicting the behavior seen in the simulations. The maximum standard error is 0.0850 and the average standard error is 0.0525.

The fractional bias [41] gives a measure of whether or not the model over or under predicts the system behavior and is given by the equation below,

$$fb = \frac{2(\overline{C^*} - \overline{C_m^*})}{(\overline{C^*} + \overline{C_m^*})}.$$

When $fb > 0$, the model under predicts $C^*$and when $fb < 0$, the model is over predicting C^*. The result of the fractional bias for each of the simulations is given in Table 5. In the table a number of positive and negative values for the fractional bias can be seen, meaning that the model both over and under predicts C^*.

In Figure 24 the model and simulation data for five different cases have been plotted to give a sample of how well the model fits the simulation data. The black data show the case of a 3 second injection time and 7 m/s vent exit speed. The magenta

Table 4. Standard Error for Nondimensional Model

	Wind Speed						
Injection Time		2m/s	3m/s	4m/s	5m/s	6m/s	7m/s
	0.5 sec	0.0850	0.0232	0.0344	0.0663	0.0629	0.0445
	1 sec	0.0838	0.0300	0.0385	0.0555	0.0522	0.0563
	1.5 sec	0.0713	0.0448	0.0415	0.0422	0.0250	0.0552
	2 sec	0.0512	0.0491	0.0443	0.0344	0.0540	0.0598
	3sec	0.0558	0.0553	0.0453	0.0639	0.0659	0.0828

Table 5. Fractional Bias for Model

Wind Speed							
Injection time		2m/s	3m/s	4m/s	5m/s	6m/s	7m/s
	0.5 sec	-0.4483	-0.0907	-0.0107	-0.0213	0.0405	0.1362
	1 sec	-0.2028	0.0513	0.0676	0.0177	0.1161	0.1311
	1.5 sec	-0.1240	0.0534	0.0798	0.0111	0.0236	0.0831
	2 sec	-0.0812	0.0755	0.0757	-0.0112	0.0089	0.0313
	3 sec	-0.0839	0.0330	0.0055	-0.0506	-0.0325	0.0019

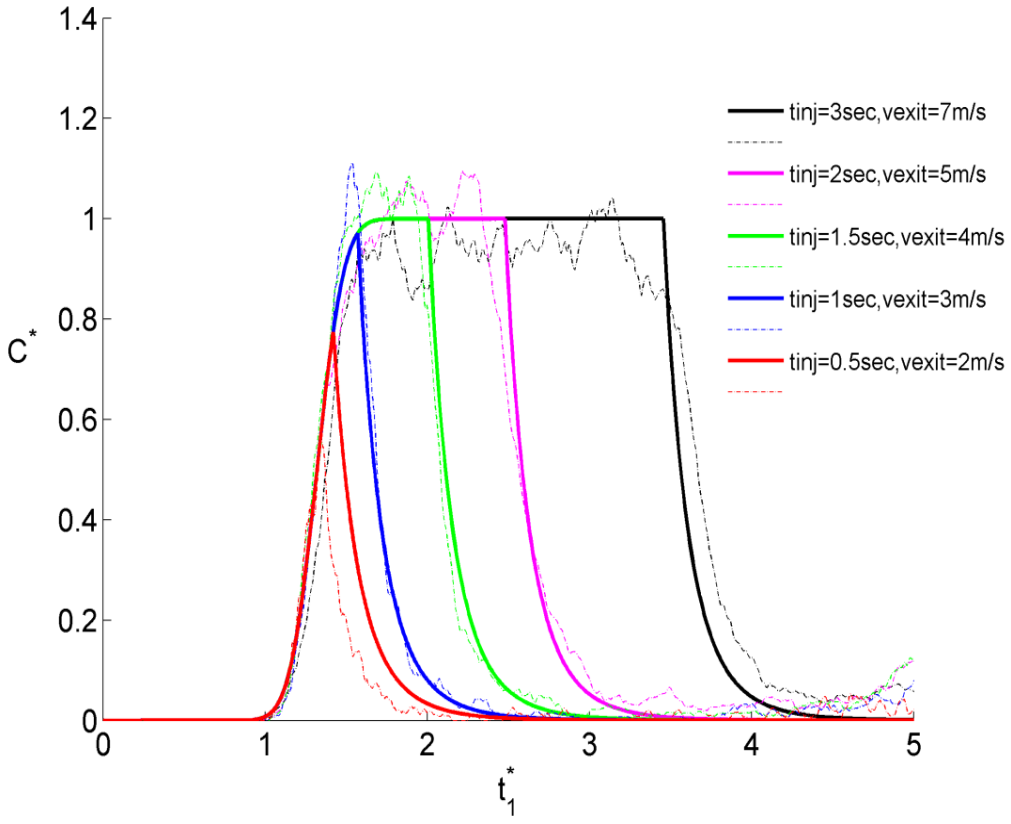

Figure 24. Simulation and model plotted for different wind speeds and injection times.

data shows for the case of a 2 second injection time and 5 m/s vent exit speed. The green data shows the case of a 1.5 second injection time and 4 m/s vent exit speed. The blue data shows the case of a 1 second injection time and 3 m/s vent exit speed. The red data shows the case of a 0.5 second injection time and 2 m/s vent exit speed.

3.5 Discussion

The CFD simulations showed that the scent particles would reach the user's position. They also showed how the concentration of scent particles changes at the user's position with time.

This concentration behavior can then be nondimensionalized to try to collapse the different system behaviors based on wind speed and injection time into one general behavior. This was not possible for the information obtained from the simulations. This could be due to the nonlinear nature of the system or an unknown factor that is not accounted for in the nondimensionalization. Despite this a piecewise model was developed that is able to predict the simulations.

Also the modeling process could easily be extended to include more simulations of the wind tunnel. Including more wind speeds and injection times would allow for more data points with which to develop the nondimensionalizations and the model.

CHAPTER 4

PHSYICAL STUDIES

The model created from the CFD simulations needs to be correlated and put into perspective with what is physically happening, a smoke visualization of the air flow and users studies were chosen to do this. The smoke visualizations provide a way to visually see how the air is really moving in the wind tunnel and the user studies give a measure of the air flow dynamics and a measure of the level of scent concentration needed for a user to detect an odor.

The smoke visualizations were done with a fan frequency of 15Hz and a total vent velocity of 10 m/s. There were three user studies done, for each study the wind tunnel had different operating conditions. The first study, had a fan frequency of 15Hz and a total vent velocity of 10 m/s, the second, had a fan frequency of 18Hz and total vent velocity of 10 m/s, and the third, had a fan frequency of 11Hz and a total vent velocity of 5 m/s. By having different operating conditions, we could compare the model to more varied physical data.

The different operating conditions of the wind tunnel produced different flows for each study. The differences in the flows can be seen in Table 6, which reports the mean and standard deviation of the wind speed and valve angles for both air inlets. It also

reports the mean and standard deviation of the wind speed, the V and U components of the wind speed and the wind angle at the user's position, with no subject present in the wind tunnel. The V component of the wind speed is the measured wind speed coming from the front screen and the U component is the measured wind speed perpendicular to the V component. Another measure of the flow is the turbulence intensity, which is the standard deviation of the wind component divided by the mean wind speed. Table 7 reports the turbulence intensity for the V and U components for each of the different studies.

Table 6. Air flow characteristics measured at the air inlet and user position, no subject present.

	Study 1		Study 2		Study 3	
	Mean	Standard Deviation	Mean	Standard Deviation	Mean	Standard Deviation
Left Valve Angle (deg)	55.697	1.744	41.253	0.693	48.319	0.357
Left Velocity (m/s)	4.968	0.262	4.930	0.200	2.186	0.162
Right Valve Angle (deg)	58.551	0.950	42.667	0.435	50.549	0.361
Right Velocity (m/s)	5.031	0.196	5.070	0.100	2.021	0.173
User's Position Wind Speed (m/s)	1.415	0.276	1.677	0.257	0.979	0.179
User's Position Wind Angle (deg)	-0.778	4.212	0.435	3.093	0.630	5.759
V (m/s)	1.436	0.547	1.689	0.460	0.967	0.382
U (m/s)	0.008	0.339	-0.015	0.287	-0.012	0.249

Table 7. Turbulence intensity for the U and V components of the wind flow at the user's position.

Turbulence Intensity	V	U
Study 1	0.387	0.240
Study 2	0.274	0.171
Study 3	0.390	0.254

4.1 Smoke Visualizations

The first objective of the simulations was to determine if the scent particles would reach the user and in Figure 14 we saw that the particles will reach the user. The smoke visualizations provide a physical way of verifying the result found in Figure 14.

The smoke visualizations were done by injecting theater fog, into the air flow. This allows the air to carry the fog through the wind tunnel. At the same time the fog is illuminated along a horizontal plane by a sheet of laser light. A camera is used to capture the flow of the illuminated fog. The sheet of laser light is generated by shining a laser beam on to a rotating disk with multiple sides. As the disk rotates at a very high speed, approximately 12000 RPM, the laser is swept across the horizontal plane and because this is happening so fast a sheet of light is generated. The captured images from the videos have very low light, requiring some image processing to show the movement of the fog through the wind tunnel.

4.1.1 Results

In Figure 25 the smoke visualization for a short period of time is given. It shows the progression of a pulse of fog. The progression of the fog is like the progression of the simulated scent particles in Figure 14. The fog follows wind along the screens then away from the screens towards the user as the wind is deflected into the room. One big difference from the simulation is the air in the physical system is much more turbulent; this turbulence is manifest in the way the fog moves toward the user in a very irregular way. The time stamp of each frame comes from the time stamp of the video and the frames per second. The videos had a frame rate of 15fps.

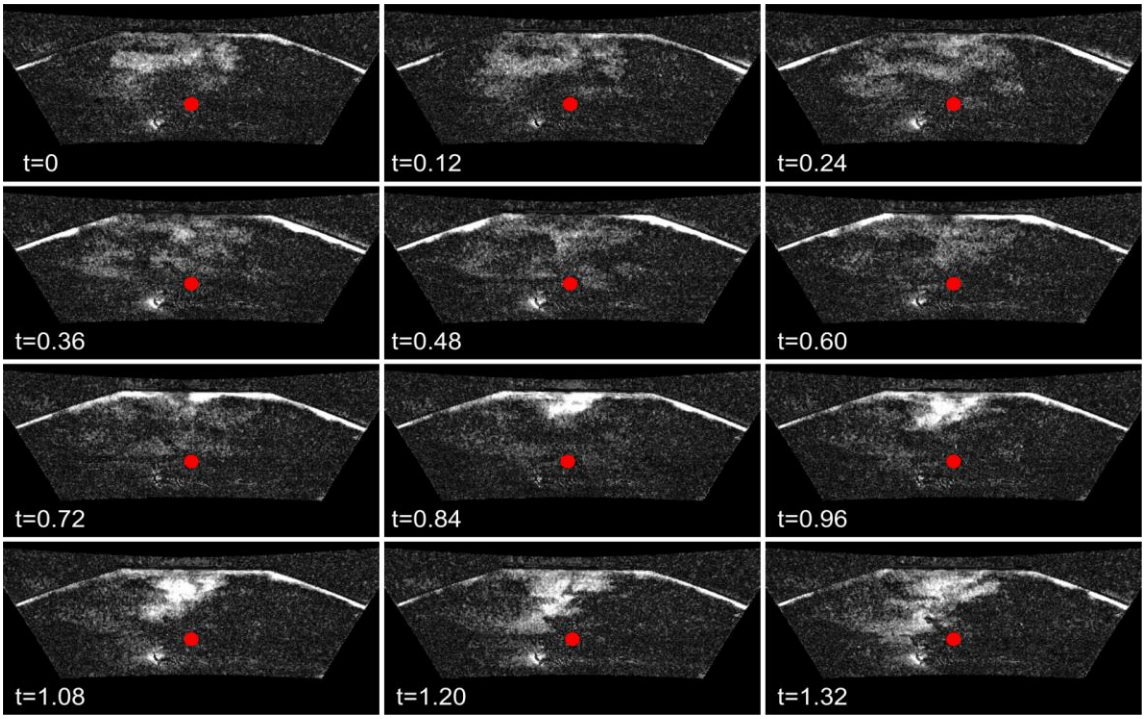

Figure 25. Smoke visualization pictures. The time stamp in seconds is based on the number of frames that elapse and the frame rate of 15fps.

4.1.2 Discussion

From Figure 25 we see that particles injected into the air stream at the air inlets will travel to the user's position and that it takes roughly 1.33 seconds for the fog to travel the distance from the injection point to the user's position. These results show that like in Figure 14 the particles will reach the users position. To compare these results to the simulations would not be advisable because the size of the smoke particles and the velocity at which they were injected into the air stream are unknown.

4.2 User Studies

The user studies were designed to determine two things about the flow dynamics; how long it takes the wind to transport the scent particles, the delay time, how much the scent particles have spread out by the time they reach the user's position, the residence time. They are also used to find a minimum amount of scent needed for a user to be able to sense the odor, this is called the minimum on time. The user experiments also provide a feel for the performance of the olfactory display.

To get a broader feel for the minimum on time, delay time, residence time and general performance of the display, three operating conditions were chosen. These operating conditions are; 15Hz fan frequency and 10 m/s total vent velocity, 18Hz fan frequency and 10 m/s total vent velocity, and 11Hz fan frequency and 5 m/s total vent velocity.

To determine the delay time, the time at which the scent is released into the air stream must be known, as well as the time at which the subject first detects the scent particles. Then, to determine the residence time, the points at which the user starts and

stops smelling the odors must be known. Consider Figure 26, which shows a model of the temporal behavior of the concentration at the user's position. The points d and e respectively represent the points at which a user would begin and end smelling an odor. By knowing the time at which these events happen, along with the knowledge of when the solenoid is turned on, the delay time and residence time can be found. The method for finding these times is described in the next section.

To find a minimum time the solenoid must be on for the subjects to sense an odor a threshold for the user must be found. This threshold is found using a staircase technique

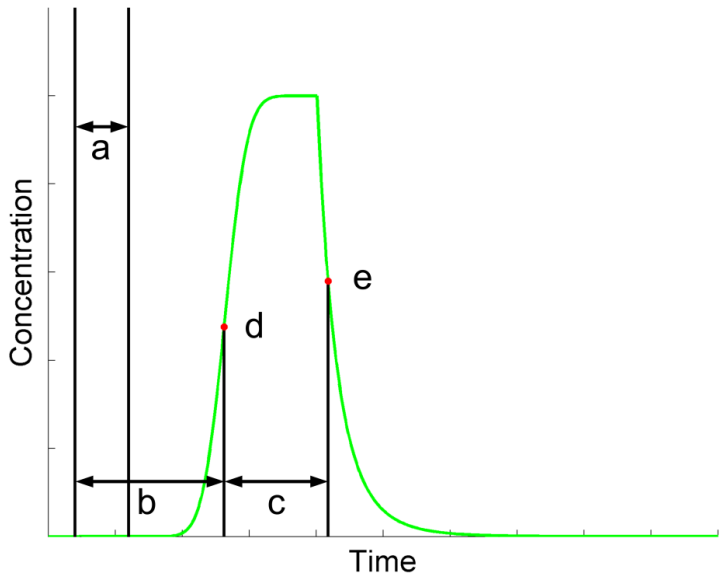

Figure 26. Representation of the concentration behavior; a) solenoid on time, b) delay time, c) residence time, d) time to first smell odor, e) time when smell is no longer noticeable.

which increases and decreases the amount of time that the solenoids are turned on. The specifics of how the staircase technique is discussed in the next section.

All of the experiments done in the user studies were exploratory in nature. Relatives, friends and lab mates made up the population of the subjects tested. For the first and second studies, there were 12 subjects, 6 male and 6 female. The third study had 6 subjects 3 female and 3 male. Information about the height and age for the subjects is given in Table 8. In the first and second studies, one subject reported being congested, and one reported being congested in the third study. Although these subjects were congested, their results were included in the analysis.

4.2.1 Experimental Setup

At the beginning of the experiment, the subjects were given a button and instructed to press down on the button when they sensed an odor, and to keep the button held down until they could no longer smell an odor. Using the same DS1103 that is used to control the solenoids, the state of the button as well as the state of the solenoid is recorded. This allows us to then calculate the delay and residence time. Figure 27 shows

Table 8. Subject statistics for height and age.

	Studies 1 & 2		Study 3	
	Height (feet)	Age (years)	Height (feet)	Age (years)
mean	5.58	25.83	5.61	26.83
std	0.25	3.48	0.31	3.98
max	6	34	6	34
min	5.17	23	5.17	23

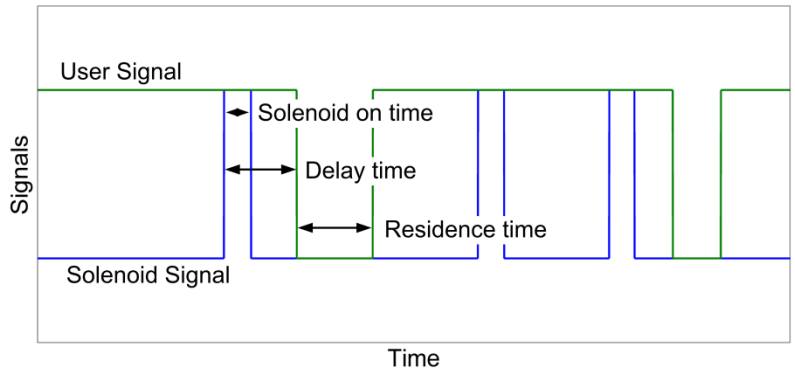

Figure 27. Sample of the binary recorded user and solenoid experimental data.

a sample of what the signals for the button and the solenoid look like. For the user signal with a value of one, it means that no scent is detected and for a value of zero it means, the user can smell an odor. For the solenoid signal a value of one means that the solenoid is on while a value of zero means that it is off.

To find the minimum on time, a staircase method of finding thresholds is executed by injecting scent pules into the air stream and depending on if the user detects the odor the solenoid's on time is increased or decreased. To determine if the solenoid's on time is to be increased or decreased, the program running the experiment waits for 6 seconds looking for the user to push the button before starting a new pulse, if the user pushes the button down in this time frame the program waits until 6 seconds after the button has been released before injecting the next pulse of scent into the air. If the scent is detected the solenoid on time is decreased by 0.1 seconds and vice versa if the scent is not detected the solenoids on time is increased by 0.1 seconds. The experiment is allowed to run for approximately 300 seconds.

4.2.2 Experimental Results

Due to the nonlinear nature of the TPAWT, the wind generated has quite a bit of turbulence in it, which can be seen in the smoke visualizations and in the measurements of the wind speed and wind angle at the user position. The wind speed and angle measurements for all of the subjects as well as a lumped value for all the subjects for each of the user studies is given in Table 9-Table 11. The turbulent nature of the wind can cause variability in the responses of the users. Another cause of variability in the results is the subjects themselves. Because everyone is different, the levels at which scents are perceived are different and variability is introduced. Other causes of variability are due to subject response time and the timing of the scent particles reaching the user with their breathing. The hope is that by including enough people in the study the variability will be mitigated and clear trends will appear.

The results have been divided into three sections; section 4.2.2.1 covers the on time results, section 4.2.2.2 covers delay time and then in section 0 the results for residence time are covered.

4.2.2.1 On Time

The minimum time that the solenoid must be on for a given fan frequency is important because it provides a measure of the minimum amount of scent required for the user to detect an odor. By doing this for a group of people and combining the results we can get a single on time that will work as a minimum amount for the whole group. The on time results for the studies are given in Figure 28, Figure 29 and, Figure 30. The on time

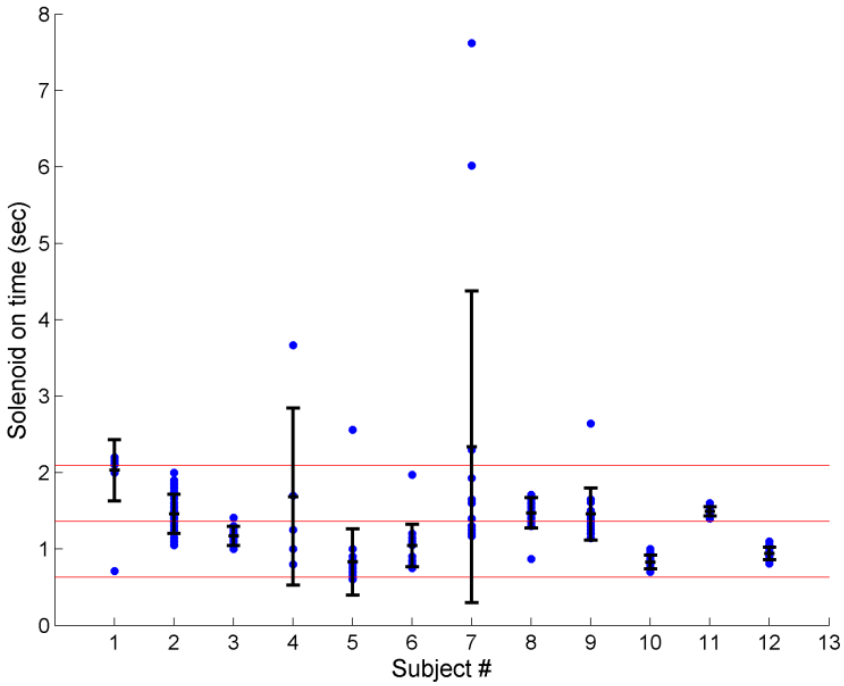

Figure 28. Experimental data of solenoid on time for the first study. The blue dots represent actual data points, black bars represent mean and standard deviation for each subject and red lines the mean and standard deviation for entire data set.

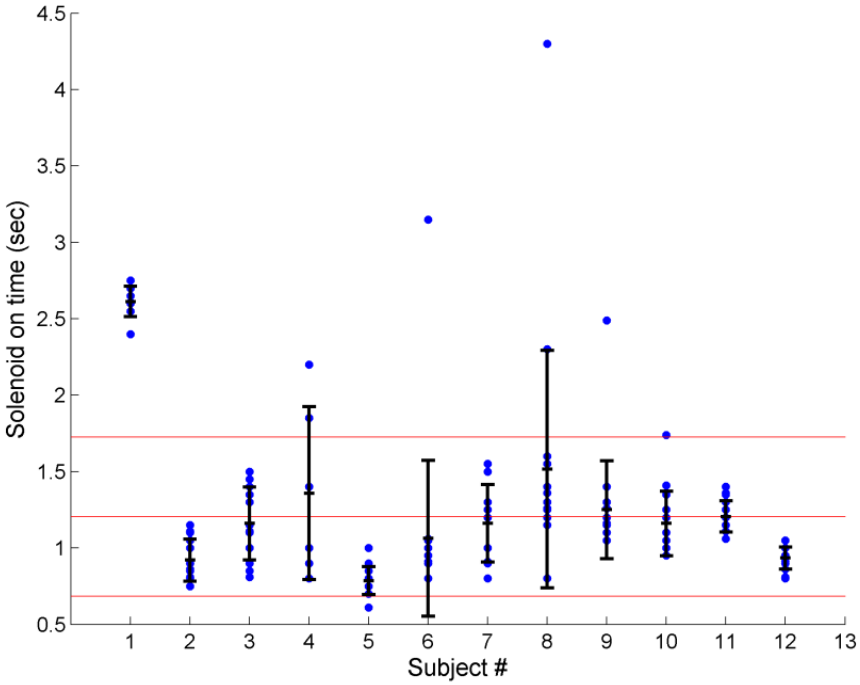

Figure 29. Experimental data of solenoid on time for the second study. The blue dots represent actual data points, black bars represent mean and standard deviation for each subject and red lines the mean and standard deviation for entire data set.

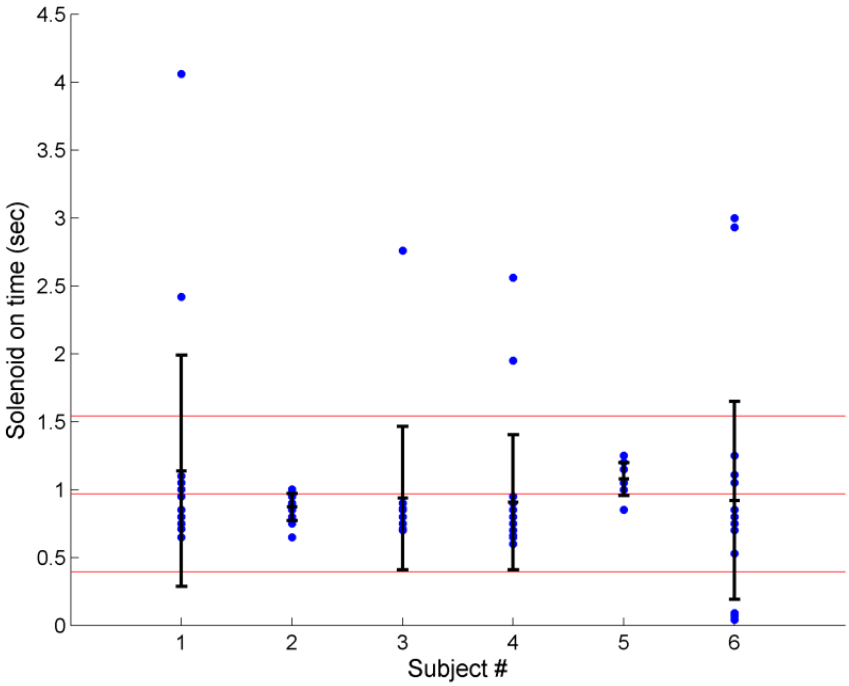

Figure 30. Experimental data of solenoid on time for the third study. The blue dots represent actual data points, black bars represent mean and standard deviation for each subject and red lines the mean and standard deviation for entire data set.

Table 9. Measured wind speed (m/s) and wind angle (deg) at the user's position for each subject's experiment, for study 1.

	Wind Speed(m/s)		Wind Angle(deg)	
Subject	Mean	Standard Deviation	Mean	Standard Deviation
1	1.050	0.165	-0.193	5.954
2	1.143	0.168	-0.254	3.706
3	1.026	0.168	-0.274	4.043
4	1.051	0.215	-0.502	6.569
5	1.441	0.208	-2.497	2.912
6	1.063	0.222	-0.570	4.868
7	0.936	0.166	6.757	6.483
8	1.551	0.174	0.417	3.269
9	1.048	0.197	-0.137	4.386
10	1.204	0.185	-0.531	4.764
11	1.016	0.121	0.379	4.251
12	1.196	0.210	-0.586	3.817
All subject average	1.126	0.249	0.675	5.594

Table 10. Measured wind speed (m/s) and wind angle (deg) at the user's position for each subject's experiment, for study 3.

	Wind Speed		Wind Angle	
Subject	Mean	Standard Deviation	Mean	Standard Deviation
1	1.244	0.453	11.393	9.900
2	1.283	0.337	11.208	6.530
3	1.502	0.355	16.189	4.667
4	1.023	0.286	6.059	10.032
5	1.337	0.450	11.715	4.525
6	1.512	0.344	19.696	7.100
7	1.362	0.349	10.788	7.154
8	1.362	0.339	12.057	4.553
9	1.340	0.393	10.432	9.331
10	1.337	0.372	17.775	9.661
11	1.328	0.251	3.655	5.882
12	1.307	0.385	9.603	8.639
All subject average	1.312	0.385	11.710	9.102

Table 11. Measured wind speed (m/s) and wind angle (deg) at the user's position for each subject's experiment, for the third user study.

	Wind Speed		Wind Angle	
Subject	Mean	Standard Deviation	Mean	Standard Deviation
1	0.883	0.102	-2.348	4.094
2	0.960	0.103	-0.997	2.934
3	0.772	0.091	3.489	4.895
4	0.910	0.101	-0.231	3.675
5	0.992	0.071	0.610	2.864
6	0.882	0.108	1.959	4.091
All subject average	0.900	0.119	0.408	4.274

mean and standard deviations for the individual subjects are marked in black. The red lines represent the mean and standard deviation for all the subject data lumped together. The mean and standard deviation information for the individuals and the group are given in Table 12

In Figure 28 for the first study, comparing the lumped mean and standard deviation compared to the individual mean and standard deviation it can be seen that the lumped mean and standard deviation fit the individual data sets well. In determining an on time for the group at this fan frequency an on time the lumped mean plus one standard deviation would ensure that all the subjects would be able to sense the odor.

In Figure 29 for the second study, the lumped mean and standard deviation does not do as good of a job of encompassing all of the individual responses. The first subject's data set doesn't fit within the bounds set by the lumped standard deviation. So picking an on time for the group based on the lumped mean and standard deviation would

Table 12. Means and standard deviations of solenoid on time, for the different studies.

	Study 1		Study 2		Study 3	
subject	Mean	Standard Deviation	Mean	Standard Deviation	Mean	Standard Deviation
1	2.029	0.400	2.612	0.099	1.138	0.852
2	1.457	0.256	0.920	0.138	0.871	0.098
3	1.169	0.125	1.160	0.240	0.938	0.527
4	1.684	1.160	1.358	0.566	0.906	0.497
5	0.831	0.434	0.785	0.091	1.077	0.121
6	1.044	0.277	1.063	0.510	0.919	0.728
7	2.338	2.041	1.161	0.255		
8	1.472	0.197	1.516	0.778		
9	1.457	0.340	1.251	0.320		
10	0.826	0.090	1.160	0.212		
11	1.493	0.059	1.206	0.102		
12	0.941	0.083	0.934	0.073		
All subject average	1.361	0.733	1.205	0.521	0.968	0.574

not ensure that all the users would be able to detect the odor. An alternative would be to use the first subject's data to pick the on time.

In Figure 30 the lumped mean and standard deviation for the third study again does an alright job of encompassing the individual responses and choosing an on time of the mean plus on standard deviation would ensure that all of these subject would detect an odor.

4.2.2.2 Delay Time

The delay time is based on the velocity of the wind. Since the wind velocities for the first and second studies are close, we would expect to have similar results. With the wind speeds having so much variability, the delay time naturally has more variability which can be seen in the standard deviations of the delay time results.

In Figure 31 the delay times for the first study are given, the individual responses vary significantly with the magnitudes of the standard deviations around the means changing a lot. Figure 32 gives the delay times for the second study. For this fan frequency the magnitudes of the standard deviations do not vary as much. Figure 33 shows the delay times for the third study. Table 13 reports the delay time results.

The seeming differences in responses between the first two studies suggest that while the wind velocities are similar there is something different about the air flow that changes how the delay time behaves.

4.2.2.3 Residence Time

The residence time is a little different from the solenoid on time and delay time. When it is assumed that the wind speed is constant the residence time is only a function of the injection time. The residence time versus injection time for the three user studies are given in Figure 34, Figure 35, and Figure 36. In Figure 34 the residence time increases gradually before plateauing, whereas in Figure 35 the residence time increases much quicker before plateauing. For the third study, Figure 36 shows a constant increase without any plateauing. The means and standard deviations for all of the different

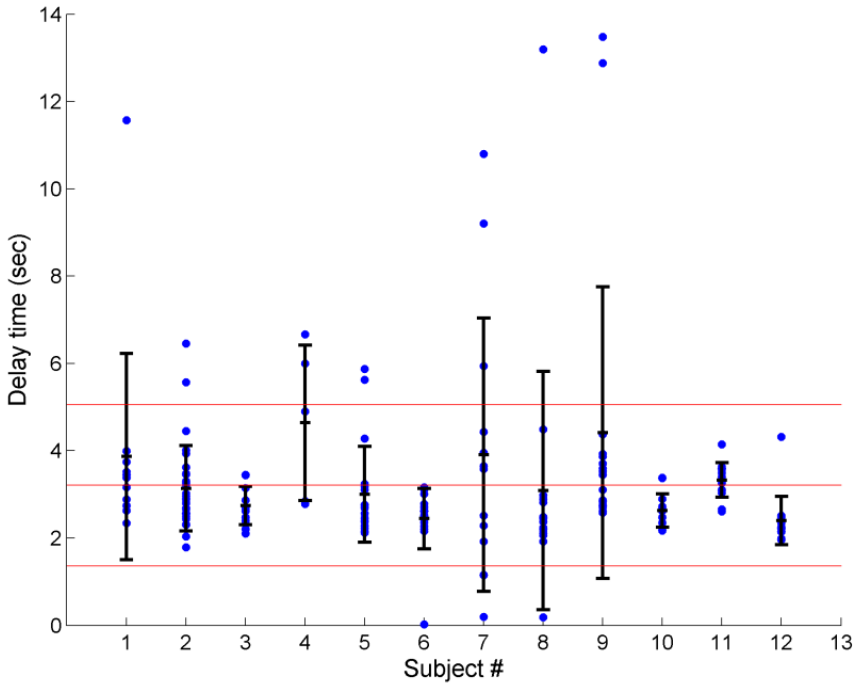

Figure 31. Experimental data of delay times for the first study. The blue dots represent actual data points, black bars represent mean and standard deviation for each subject and red lines the mean and standard deviation for entire data set.

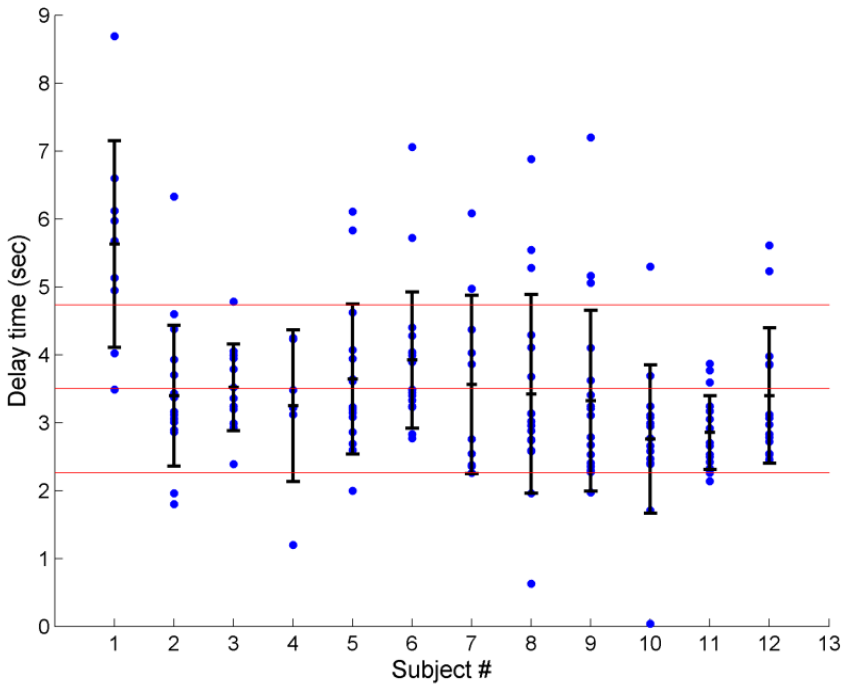

Figure 32. Experimental data of delay times for the second study. The blue dots represent actual data points, black bars represent mean and standard deviation for each subject and red lines the mean and standard deviation for entire data set.

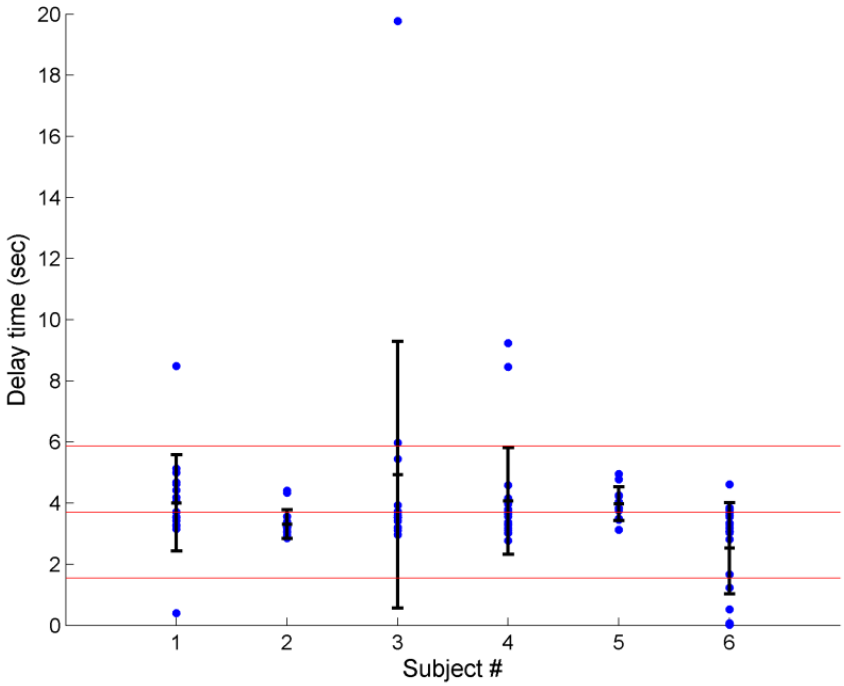

Figure 33. Experimental data of delay times for the third study. The blue dots represent actual data points, black bars represent mean and standard deviation for each subject and red lines the mean and standard deviation for entire data set.

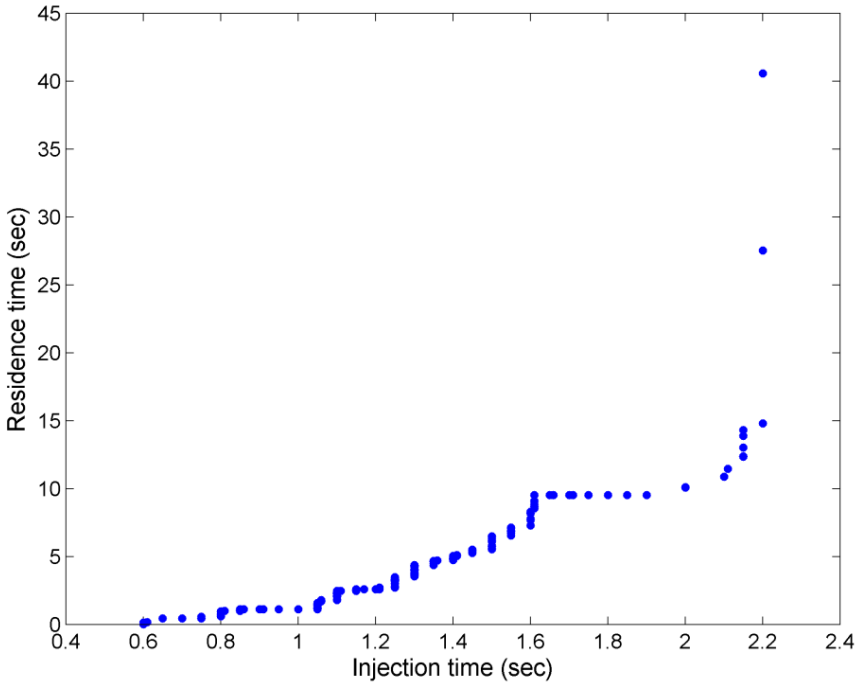

Figure 34. Residence time as a function of injection time, for the first study. Some injection times where sensed more often, leading to more data points for some injection times.

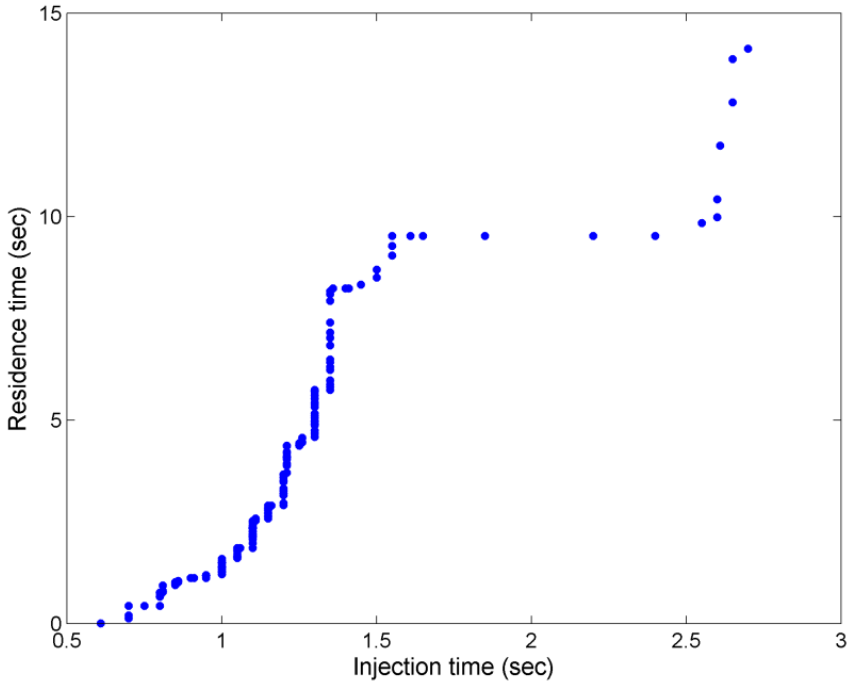

Figure 35. Residence time as a function of injection time, for the second study. Some injection times where sensed more leading to more data points for some injection times.

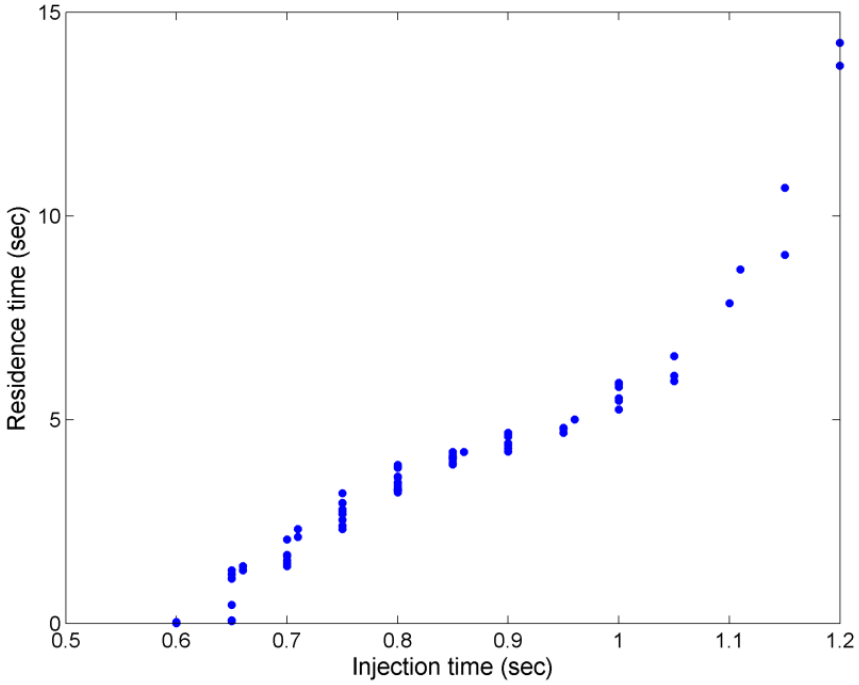

Figure 36. Residence time as a function of injection time, for the third study. Some injection times where sensed more leading to more data points for some injection times.

Table 13. Mean and standard deviation of delay time, for the different studies.

	Study 1		Study 2		Study 3	
subject	Mean	Standard Deviation	Mean	Standard Deviation	Mean	Standard Deviation
1	3.867	2.361	5.628	1.523	4.005	1.574
2	3.135	0.978	3.395	1.036	3.312	0.468
3	2.745	0.436	3.517	0.637	4.926	4.359
4	4.640	1.782	3.250	1.117	4.069	1.745
5	3.001	1.096	3.641	1.105	3.979	0.552
6	2.446	0.691	3.921	1.005	2.525	1.496
7	3.907	3.129	3.561	1.313		
8	3.090	2.730	3.421	1.464		
9	4.414	3.344	3.322	1.332		
10	2.628	0.385	2.759	1.094		
11	3.330	0.394	2.853	0.544		
12	2.400	0.556	3.397	0.996		
All subject average	3.209	1.849	3.497	1.239	3.708	2.162

injection times for the user studies are given in Table 14, Table 15, and Table 16. When considering the data in these tables, some of the injection times had more data points associated with them, meaning that more of the subjects recognized an odor with this injection time.

4.2.3 Model Correlation

In the correlation of the model to the user experiments, three different estimates of where on the C^* curve the user would start and stop smelling the odor are used. These estimates are 0.25, 0.50, and 0.75 C^*.

Table 14. Residence times for study 1.

Injection Time (s)	Mean (s)	Standard Deviation (s)	# of data points
0.6	0.070	0.085	2
0.61	0.180	NA	1
0.65	0.430	0.000	5
0.7	0.430	0.000	4
0.75	0.478	0.066	4
0.8	0.831	0.160	8
0.81	1.000	0.000	2
0.85	1.066	0.049	8
0.86	1.120	0.000	2
0.9	1.120	0.000	8
0.91	1.120	NA	1
0.95	1.120	0.000	3
1	1.120	0.000	7
1.05	1.326	0.156	32
1.06	1.750	0.038	4
1.1	2.003	0.212	52
1.11	2.480	NA	1
1.15	2.513	0.037	34
1.17	2.580	NA	1
1.2	2.580	0.000	4
1.21	2.627	0.069	16
1.25	3.052	0.290	24
1.3	4.055	0.263	31

Injection Time (s)	Mean (s)	Standard Deviation (s)	# of data points
1.35	4.446	0.121	17
1.36	4.700	NA	1
1.4	4.861	0.111	8
1.41	5.080	0.042	2
1.45	5.372	0.107	9
1.5	6.026	0.356	9
1.55	6.867	0.185	8
1.6	7.961	0.388	7
1.61	8.927	0.402	8
1.65	9.520	0.000	8
1.66	9.520	NA	1
1.7	9.520	0.000	2
1.71	9.520	NA	1
1.75	9.520	NA	1
1.8	9.520	0.000	2
1.85	9.520	NA	1
1.9	9.530	NA	1
2	10.095	0.021	2
2.1	10.860	NA	1
2.11	11.460	0.014	2
2.15	13.188	0.889	5
2.2	27.643	12.885	3

Table 15. Residence times for study 2.

Injection Time (s)	Mean (s)	Standard Deviation (s)	# of data points
0.61	0.010	NA	1
0.7	0.330	0.288	3
0.75	0.723	0.041	6
0.8	0.858	0.109	12
0.81	1.090	0.068	4
0.85	1.200	0.018	4
0.86	1.260	0.000	2
0.9	1.352	0.052	9
0.91	1.510	0.019	5
0.95	1.697	0.112	13
1	2.246	0.098	29
1.05	2.598	0.137	12
1.06	2.730	0.000	4
1.1	2.787	0.048	7
1.11	2.916	0.025	5
1.15	3.415	0.202	15
1.16	3.880	NA	1
1.2	4.176	0.166	14

Injection Time (s)	Mean (s)	Standard Deviation (s)	# of data points
1.25	4.413	0.022	6
1.26	4.580	0.014	2
1.3	4.888	0.127	8
1.35	5.270	0.127	5
1.36	5.520	0.095	3
1.4	5.708	0.051	6
1.41	5.820	NA	1
1.45	5.925	0.078	2
1.5	6.253	0.040	3
1.55	7.519	0.712	12
1.85	8.240	NA	1
2.2	8.355	0.239	14
2.4	9.280	NA	1
2.55	9.840	NA	1
2.6	10.200	0.311	2
2.61	11.740	NA	1
2.65	13.340	0.750	2
2.7	14.130	NA	1

Table 16. Residence times for study 3.

Injection Time (s)	Mean (s)	Standard Deviation (s)	# of data points
0.6	0.020	0.012	5
0.65	0.609	0.573	7
0.66	1.373	0.064	3
0.7	1.635	0.232	6
0.71	2.220	0.141	2
0.75	2.742	0.297	12
0.8	3.444	0.218	18
0.85	4.060	0.095	9
0.86	4.210	0.000	2

Injection Time (s)	Mean (s)	Standard Deviation (s)	# of data points
0.9	4.468	0.168	10
0.95	4.746	0.062	7
0.96	5.010	NA	1
1	5.563	0.218	11
1.05	6.197	0.321	3
1.1	7.860	NA	1
1.11	8.690	NA	1
1.15	9.865	1.167	2
1.2	13.970	0.396	2

Before the delay time and residence time can be correlated to the model, they must first be transformed into the nondimensional space. The nondimensionalization comes from Chapter 3 and requires the effective velocity. The effective velocity is calculated by dividing the distance s, the distance the particles travel, by the mean lumped measured delay times for the different fan frequencies found in Table 13. This gives effective velocities of 1.639 m/s for study one, 1.504 m/s for study two, and 1.418 m/s for study three.

To compare the model to the study results there are three options; the first is to compare the study results to the model that matches air inlets velocity the closest, the second, is to use the model that matches the user position velocity the closest, and lastly, is to use the model that matches the effective velocity the best. The option that fits the best is to use the model that matches the effective velocity.

Section 4.2.3.1 gives the delay time correlation and section 0 gives the correlation for the residence time.

4.2.3.1 Delay Time

To understand how well the model does at predicting the nondimensional delay time the measured nondimensional delay times are plotted relative to the estimates, and are found in Figure 37, Figure 38, and Figure 39. In the figures the model of C^* is shown in blue, the data points are the red dots and the black line represents the mean nondimensional delay and the dashed black line represents the standard deviation of the nondimensional delay. These figures show that the model over predicts the time it will

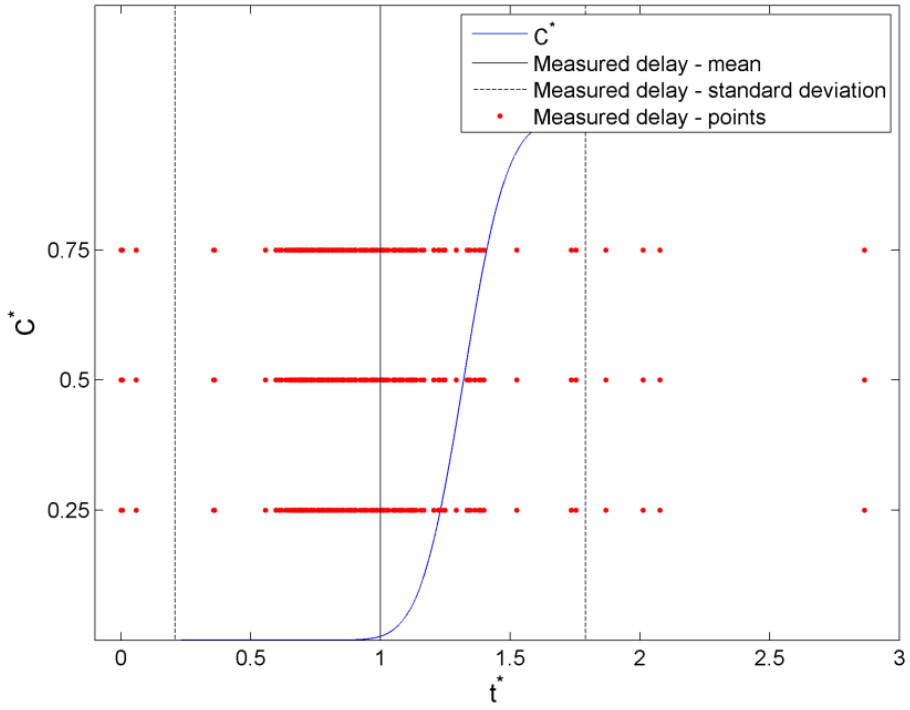

Figure 37. Predicted rising edge of the model plotted with measured delay times at the different estimates of C^*, for the second study.

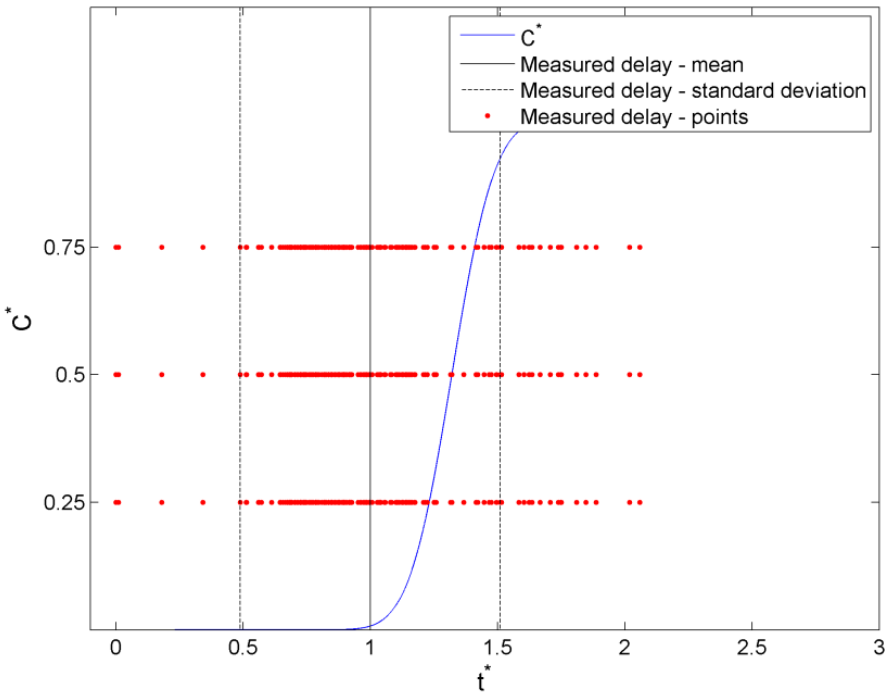

Figure 38. Predicted rising edge of the model plotted with measured delay times at the different estimates of C^*, for the first study.

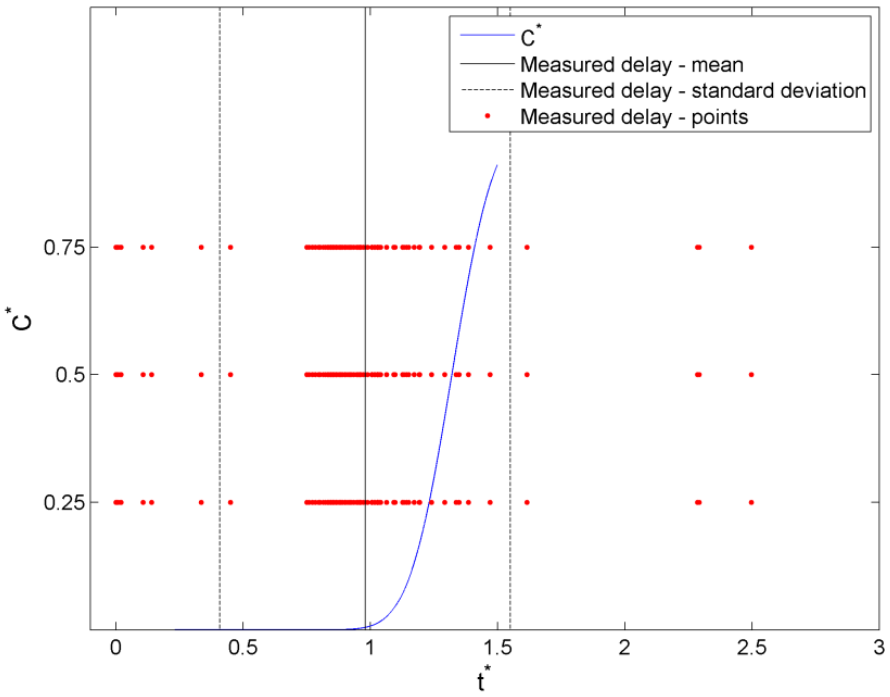

Figure 39. Predicted rising edge of the model plotted with measured delay times at the different estimates of C^*, for the third study.

take for the particles reach the user. However, each of the estimates is within one standard deviation for both of the fan frequencies.

This difference could be due to a couple of things, the error due to the timing of scent arrival and user breathing, error in the development of the nondimensionalization or even errors from the simulations.

4.2.3.2 Residence Time

The modeled nondimensional residence time is calculated by finding the nondimensional time when C^* is greater than the estimates of where the user starts and stops smelling, the odor. In Figure 40, Figure 41, and Figure 42 the modeled nondimensional residence times are plotted versus the measured nondimensional residence times for each of the user studies. The black line represents what would be a perfect correlation between the model and reality. These figures show that the model over and under predicts what is happening in reality, and at the extremes the model does not do a very good job of predicting what is happening. This suggests that using injection times close to where the model does a good job of predicting would be a good control strategy. Looking at the residence time information from the aspect of specific injection times, 1.1 and 1.3 seconds for the first and second user studies and 0.8 seconds for the third user study. A feel for how the model compares to the user studies can be obtained.

In Figure 43, Figure 44, and Figure 45 the models for the different user studies have been plotted then the measured mean and standard deviation of the residence time for the injection times specified above are plotted as well. In Figure 43, for an injection time of 1.1 seconds we can see that model and reality are close. However, in Figure 44

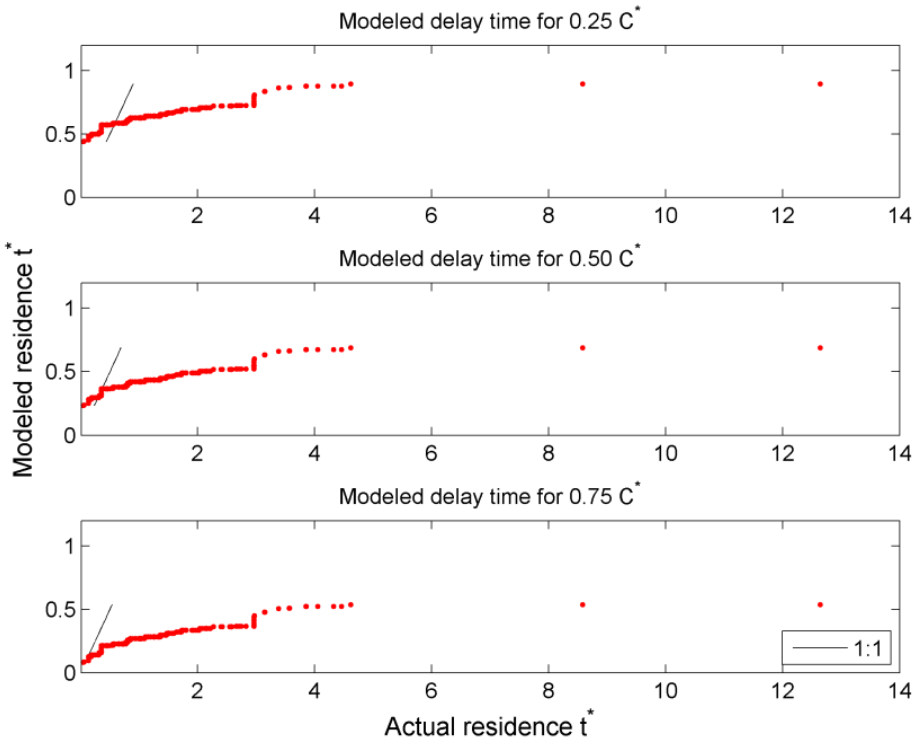

Figure 40. Predicted residence time vs. actual residence time, for the first study. The black line represents a 1:1 correlation.

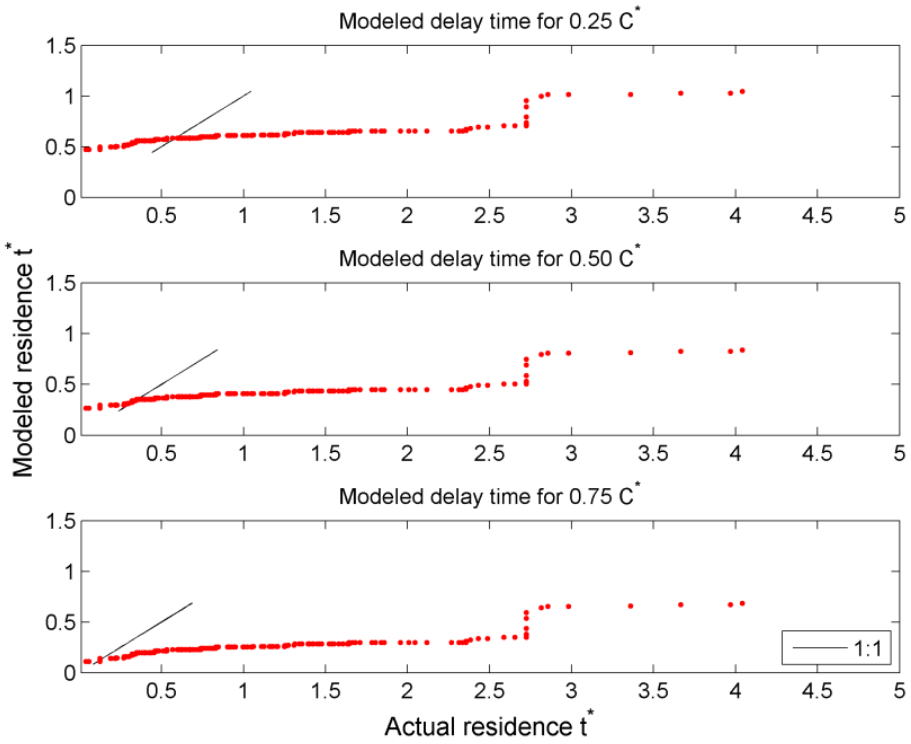

Figure 41. Predicted residence time vs. actual residence time, for the second study. The black line represents a 1:1 correlation.

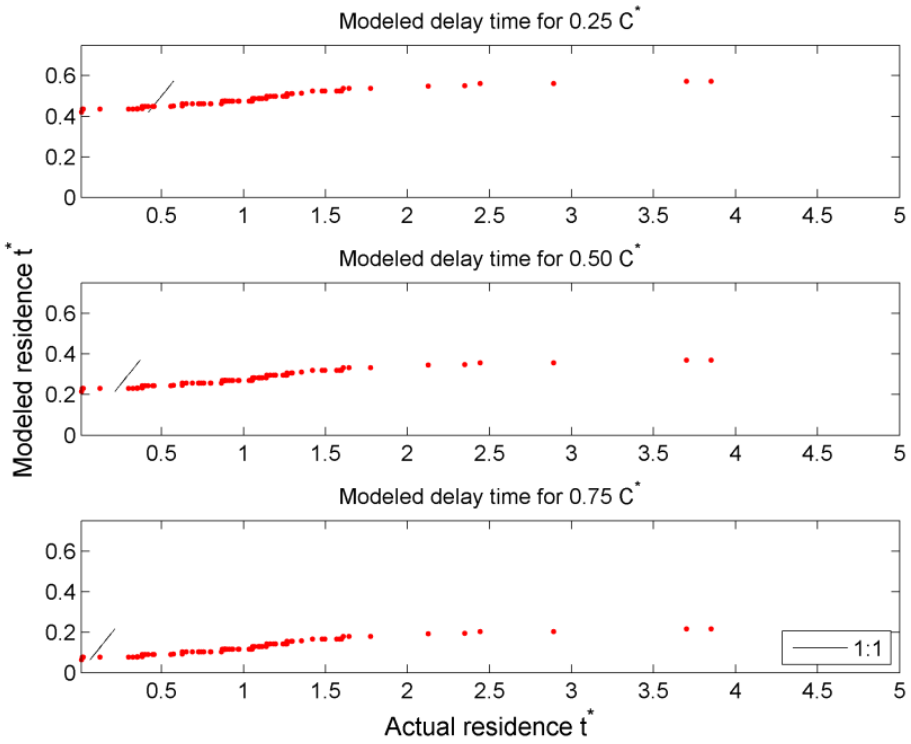

Figure 42. Predicted residence time vs. actual residence time, for the third study. The black line represents a 1:1 correlation.

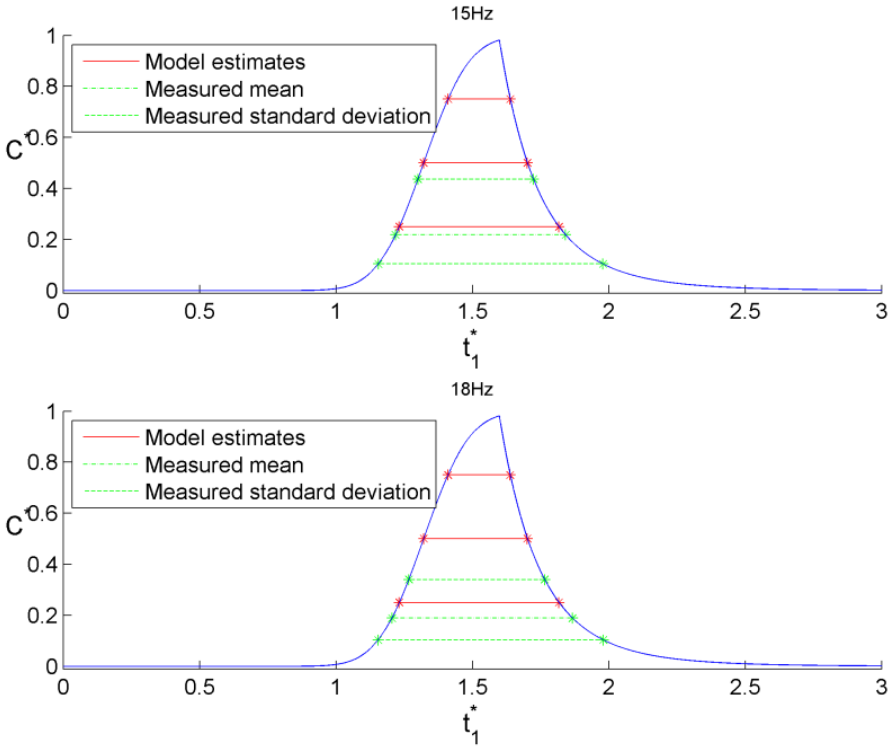

Figure 43. Nondimensional residence time estimates and measurements with a 1.1 second injection time, for the first and second user studies. The red line represents the estimates and colored lines the measurements.

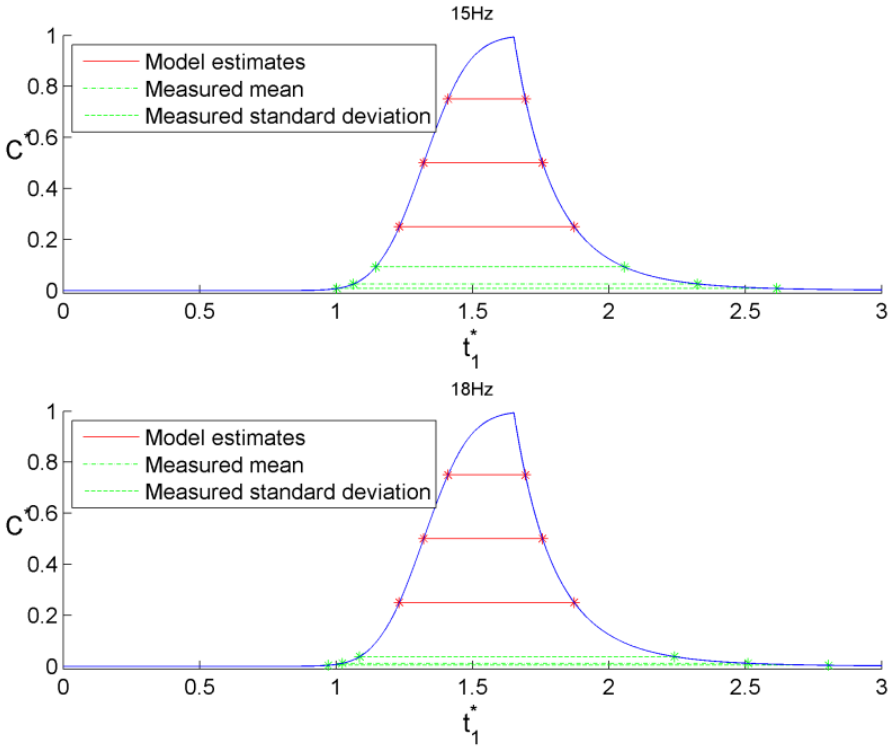

Figure 44. Nondimensional residence time estimates and measurements, with a 1.3 second injection time for the first and second user studies. The red line represents the estimates and colored lines the measurements.

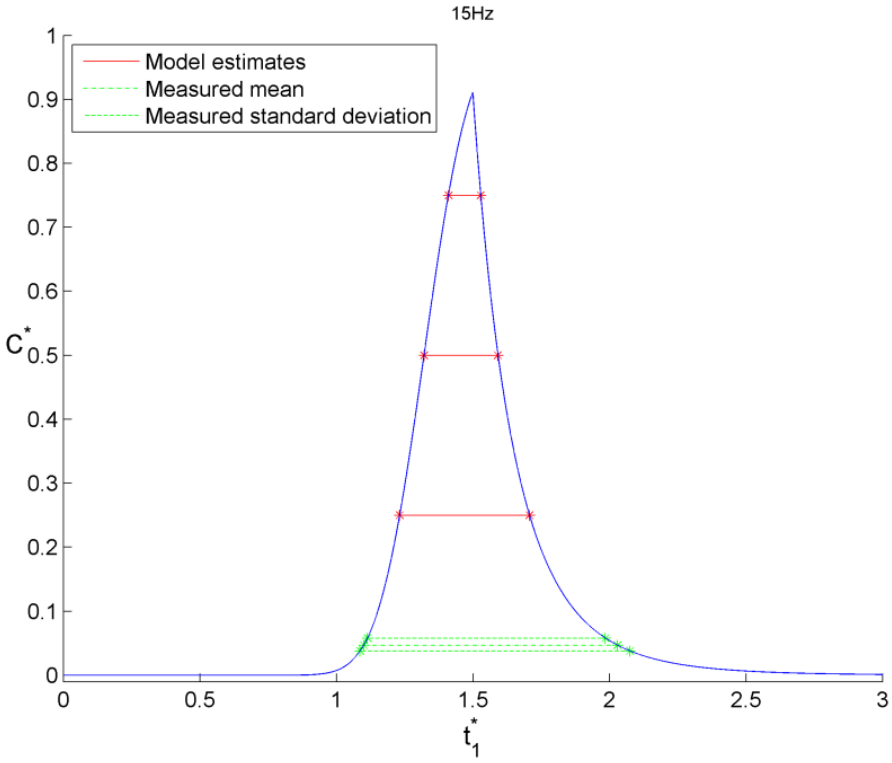

Figure 45. Nondimensional residence time estimates and measurements with a 0.8 second injection time, for the third user study. The red line represents the estimates and colored lines the measurements.

and Figure 45 the model and the measured results do not match well. This comparison is flawed, because we do not know the concentration at which the subjects begin sensing an odor. This means the placement of the measured residence times is not accurate. However, we are able to get a feeling for how the residence time compares to the model of C^*.

4.3 Discussion

The results obtained by the smoke visualizations and the user studies were able to tell us a lot about the physical system and the simulations. The smoke visualizations showed that the scent particles would be carried to the user like the simulations predicted and the user studies showed that the olfactory display is possible and that certain properties of the wind flow can be measured.

When looking at the study data, definite trends can be seen in the time it takes for the subjects to sense an odor and also the length of time that the solenoid must be on for the subjects to sense an odor. Because the first two studies had wind speeds at the user's position that are so close together, the delay times for both experiments could be considered to be a part of the same group. However, the very different residence time behaviors suggests that the small change in fan frequency changes the way the air moves enough that they cannot be considered to be a part of the same group.

When the measured properties are compared to the model developed in chapter 3 there is some correlation between the two. This suggests that there is some unknown that is causing an error in the model. This error could be due to the scent arrival and user breathing timing issues. It could also be that the simulations are not giving a totally

accurate depiction of what is physically happening. This could be due to some physical aspect of the wind tunnel is not being simulated or not being simulated well. It might also mean that the nondimensionalization of the model is missing some piece of information.

CHAPTER 5

DISCUSSION

The TPAWT provides an excellent platform for an olfactory display and the findings of this thesis show that the TPAWT's ability to generate wind provides a very effective means for transporting scents to a user. In the development of the olfactory display a method for injecting scents into the air stream of the wind tunnel was developed, as well as a model that could be used to control the concentration of the scent particles at the user. The user studies that were conducted tried to evaluate how well the model predicts the delay time and the residence time as well as give a feel for how the display works, and while the correlation between the model and reality was not firmly established, the user studies showed that the olfactory display was able to communicate smell to a person using the TPAWT. With this first iteration completed and with the knowledge gained, more work can be done to improve the olfactory display and make it a device that could be used extensively in human perception experiments.

5.1.1 Olfactory Display

The olfactory display that has been created for the UUTVE is unique because it uses the wind generated by the TPAWT to carry the scents to the user of the

environment. This allows the user to be unencumbered by a device that must be worn or have the issue of the scents lingering in the area around the user.

The future work with the olfactory display should go in a few directions. The display itself should be improved by developing a method of injecting more than one scent at a time. The current injector can inject only one scent at a time, while most other olfactory displays can emit many more than this.

Also a method of injecting the scents into the air stream that doesn't make as much noise or any noise at all should be researched and developed. The noise generated by the nozzle can be a distraction from the sense of presence in the virtual environment and should be removed. An olfactory display like Kim's [30] which uses temperature sensitive gels could be developed. Also a display using inkjet cartridges is an option. The current work being done in olfactory displays provide an excellent resource for the development of the next display.

Also, the point where the scents are injected into the air stream should be changed. Changing the position of the nozzles could improve the efficiency of the system. The nozzles are quite a long way from the user and because of the turbulent nature of the air flow more scent is required for a user to be able to sense the odor. So by moving the injection point closer to the user the amount of scent used would be decreased, because less of the scent particles would be lost to the turbulent air flow. Moving the injection points could also reduce the number of injection points. By choosing the new injection points to be in front of the user, the number of injectors would be cut in half. This is because with the injection point in front of the user there wouldn't be a need to inject scent into both air streams.

Moving the injection point would require a change in the simulations. However there may be some problems with the simulations not matching the experimental data, so changes to the simulations may be necessary anyway. One of these problems could be in the turbulence model. As was seen from the smoke visualizations and the measurements of wind speed, angle and the turbulence intensity, there is significant amount of turbulence which is not seen in the simulations and should be accounted for.

5.1.2 Simulations and Model

The CFD simulations of the particle dispersions provided useful insight into the behavior of the wind tunnel. The simulations showed that the wind would carry the particles to where the user stands and they showed how the concentration would change over time at the user's position.

From the simulations a model was developed that is able to predict the simulated concentration, with the maximum standard error equal to 0.0850 and the average standard error equal to 0.0525. While the model is able to predict the simulations it does not do the best job of predicting the physical system, there was some correlation that would seem to suggest that the simulations are getting close but, there is information that is missing. This missing information could be affecting the simulations or the development of the model based on the simulations. The information might be linked to the timing issues involved with user breathing and the arrival of the scent particles at the user's position.

If in the future, there are changes made to the injection points, the simulations will need to be changed to account for these physical changes. There may be a desire to have more simulations from which to develop the model as well.

Something that needs to be considered when doing further validation experiments is the wind speeds at which the TPAWT is operating should be significantly different from each other. This means that the wind speeds should not have standard deviations that overlap. Doing this would provide distinctly different nondimensional residence times and solenoid on times, which could then be compared to the model thus giving a better picture of the overall fit of the model, and not just the fit for a small region.

The user studies provided a very subjective uncertain picture of how the concentration behaves in the TPAWT. By employing a more objective method of measuring the delay time, residence time and concentration a more precise picture could be obtained and compared to the modeled that has been developed. One method to obtain this picture would be to inject propylene into the air stream and then measure the concentration of the propylene at various points within the TPAWT. The points at which the propylene should be measured, must take into account the three dimensional nature of the wind flow. Doing this in conjunction with simulations that measure the theoretical concentration at matching points in the TPAWT simulation would provide for a much more robust model of what is happening in the wind tunnel and would not contain the inherent inconsistencies that human subjects introduce into the results of experiments.

5.1.3 User Studies

In the user experiments people were able to sense odors and certain qualities of the air flow were measured, such as the delay time and the residence time. The experiments also determined what the minimum on time for the individuals as well as the group for the different fan frequency. This shows that the wind generation capabilities of

the TPAWT can be used to create an olfactory display. In the case of this thesis, the olfactory display created is very basic and can be thought of as a proof of concept. Table 17 shows the lumped On time and Delay time values found in the user studies.

More user experiments should be done to build on the work already done and verify the results that have been obtained. More threshold experiments for wind speeds that are significantly different should be done. Doing this would provide a method other than CFD simulations for determining how to control the olfactory display.

Also a more controlled approach should be taken in conducting further experiments. This approach should include, but not necessarily limited to the following; ensuring consistent head placement for a series of experiments, prescreening of a subjects ability to detect odors, allowing for more time in between experiments to minimize fatigue, and the thorough vetting of test subjects.

The consistent placement of a subjects head would be of benefit because it would remove one more variable that may lead to inconsistencies in the result that are obtained. Also by prescreening a subject for their ability to smell, a common base line would be

Table 17. Average over all subjects for On time and Delay time.

	Study 1		Study 2		Study 3	
	Mean	Standard Deviation	Mean	Standard Deviation	Mean	Standard Deviation
On Time (sec)	1.361	0.733	1.205	0.521	0.968	0.574
Delay Time (sec)	3.209	1.849	3.497	1.239	3.708	2.162

established by which the results of the experiment could be based upon. There are specific tests for determining a person's ability to smell that have been developed, one is

a test by the Connecticut Chemosensory Clinical Research Center (CCCRC) [42]. Another test, the so called "Sniffin' Sticks," has been developed and shown to be comparable to the CCCRC test can be purchased and used to conduct the prescreening of subjects [43]. Vetting the subjects will help in the control of the experiments by making sure that factors that would affect their ability to smell would be documented and factored into the results obtained.

The olfactory display developed for the UUTVE, has great potential it was shown that scents can be transported to a user and that a model can be developed from simulations. While the connection between the information gathered from the user studies does not correlate very well with the model, the same trends can be seen, and more effort should be put forth in trying to create a better correlation by doing more user experiments and employing more objective means of measuring aspects of the flow dynamics.

In whole it is my opinion that there is great potential for the olfactory display and that it should not be allowed to sit and that future contributions in the development of the display for the UUTVE will make the UUTVE a much better virtual environment for the training and rehabilitation of humans.

REFERENCES

[1] H. G. Hoffman, "Virtual-reality therapy," *Scientific American,* vol. 291, pp. 58-65, 2004.

[2] A. C. Lear, "Virtual reality provides real therapy," *IEEE Computer Graphics and Applications,* vol. 17, pp. 16-20, 1997.

[3] A. S. Rizzo and G. J. Kim, "A SWOT analysis of the field of virtual reality rehabilitation and therapy," *Presence,* vol. 14, pp. 119-46, 2005.

[4] H. Q. Dinh, N. Walker, L. F. Hodges, S. Chang, and A. Kobayashi, "Evaluating the importance of multi-sensory input on memory and the sense of presence in virtual environments," in *Proceedings of Virtual Reality, 13-17 March 1999*, Los Alamitos, CA, USA, 1999, pp. 222-8.

[5] C. Cruz-Neira, D. J. Sandin, and T. A. DeFanti, "Surround-screen projection-based virtual reality: the design and implementation of the CAVE," in *Proceedings of the ACM SIGGRAPH '93 Conference on Computer Graphics, Aug 1 - 6 1993*, Anaheim, CA, United states, 1993, pp. 135-142.

[6] D. I. Grow and J. M. Hollerbach, "Harness design and coupling stiffness for two-axis torso haptics," in *IEEE Virtual Reality 2006, March 25, 2006 - March 29, 2006*, Alexandria, VA, United states, 2006, p. 82.

[7] J. Hollerbach, D. Grow, and C. Parker, "Developments in locomotion interfaces," in *2005 IEEE 9th International Conference on Rehabilitation Robotics, 28 June-1 July 2005*, Piscataway, NJ, USA, 2005, pp. 522-5.

[8] S. Kulkarni, C. Fisher, E. Pardyjak, M. Minor, and J. Hollerbach, "Wind display device for locomotion interface in a virtual environment," in *2009 World Haptics Conference (WHC 2009), 18-20 March 2009*, Piscataway, NJ, USA, 2009, pp. 184-9.

[9] S. Chakravarthy, "MODELING AND CONTROL FOR SIMULATED WIND IN IMMERSIVE VIRTUAL ENVIRONMENT," Mechanical Engineering, University of Utah, Salt Lake City, 2009.

[10] A. S. Desai, "DESIGN OF VENTS F O R THE INCORPORATION OF WIND EFFECTS T O A VIRTUAL ENVIRONMENT," Mechancial Engineering, University of Utah, Salt Lake City, 2010.

[11] C. J. Fisher, "DESIGN AND CONSTRUCTION OF AN ATMOSPHERIC DISPLAY WIND TUNNEL FOR VIRTUAL REALITY USE," Mechanical Engineering, University of Utah, Salt Lake City, 2009.

[12] S. Kulkarni, "Underactuated Control and Characterization of Wind Flow in a Virtual Environment," Ph.D., Mechanical Engineering, University of Utah, Salt Lake City, 2009.

[13] E. R. Pardyjak and M. J. Brown, "Evaluation of a Fast-Response Urban Wind Model-Comparison to Single-Building Wind Tunnel Data," 2001.

[14] E. R. Pardyjak, B. Singh, A. Norgren, and P. Willemsen, "" Using video gaming technology to achieve low-cost speed up of emergency response urban dispersion simulations," 2007.

[15] P. Willemsen, A. Norgren, B. Singh, and E. Pardyjak, "" Development of a new methodology for improving urban fast response Lagrangian dispersion simulation via parallelism on the graphics processing unit."

[16] T. Nakamoto, M. Kinoshita, K. Murakami, and A. Yossiri, "Demonstration of improved olfactory display using rapidly-switching solenoid valves," in *VR 2009 - IEEE Virtual Reality 2009, March 14, 2009 - March 18, 2009*, Lafayette, LA, United states, 2009, pp. 301-302.

[17] T. Nakamoto, T. Yamanaka, and R. Matsumoto, "Olfactory display using solenoid valves controlled by delta-sigma modulation," in *Proceedings on International Conference on Multi-Sensor Fusion and Integration for Intelligent Systems, 20-22 Aug. 2001*, Dusseldorf, Germany, 2001, pp. 13-18.

[18] T. Nakamoto and K. Yoshikawa, "Movie with scents generated by olfactory display using solenoid valves," in *IEEE Virtual Reality 2006, March 25, 2006 - March 29, 2006*, Alexandria, VA, United states, 2006, p. 48.

[19] T. Nakamoto, S. Otaguro, M. Kinoshita, M. Nagahama, K. Ohinishi, and T. Ishida, "Cooking up an interactive olfactory game display," *IEEE Computer Graphics and Applications*, vol. 28, pp. 75-9, 2008.

[20] K. Sakamoto and F. Kanazawa, "Face detection for interactive tabletop viewscreen system using olfactory display," in *MIPPR 2009: Automatic Target Recognition and Image Analysis, 30 Oct.-1 Nov. 2009*, USA, 2009, p. 749515 (8 pp.).

[21] K. Sakamoto and F. Kanazawa, "Virtual vision system with actual flavor by olfactory display," in *Optoelectronic Imaging and Multimedia Technology, 18-20 Oct. 2010*, USA, 2010, p. 78501I (8 pp.).

[22] T. Yamada, S. Yokoyama, T. Tanikawa, K. Hirota, and M. Hirose, "Wearable olfactory display: Using odor in outdoor environment," in *IEEE Virtual Reality 2006, March 25, 2006 - March 29, 2006*, Alexandria, VA, United states, 2006, p. 28.

[23] H. Matsukura, A. Ohno, and H. Ishida, "Fluid dynamic considerations for realistic odor presentation using olfactory display," *Presence: Teleoperators and Virtual Environments*, vol. 19, pp. 513-526, 2010.

[24] H. Matsukura, H. Yoshida, H. Ishida, A. Saitoh, and T. Nakamoto, "Odor presentation with a vivid sense of reality: Incorporating fluid dynamics simulation into olfactory display," in *VR 2009 - IEEE Virtual Reality 2009, March 14, 2009 - March 18, 2009*, Lafayette, LA, United states, 2009, pp. 295-296.

[25] A. Kadowaki, D. Noguchi, S. Sugimoto, Y. Bannai, and K. Okada, "Development of a High-performance Olfactory Display and Measurement of Olfactory Characteristics for Pulse Ejections," in *2010 10th IEEE/IPSJ International Symposium on Applications and the Internet (SAINT), 19-23 July 2010*, Los Alamitos, CA, USA, 2010, pp. 1-6.

[26] S. Sugimoto, D. Noguchi, Y. Bannnai, and K. Okada, "Ink jet olfactory display enabling instantaneous switches of scents," in *18th ACM International Conference on Multimedia ACM Multimedia 2010, MM'10, October 25, 2010 - October 29, 2010*, Firenze, Italy, 2010, pp. 301-310.

[27] A. Kadowaki, J. Sato, K. Ohtsu, Y. Bannai, and K. Okada, "Pulse ejection presentation system synchronized with breathing," *Electrical Engineering in Japan (English translation of Denki Gakkai Ronbunshi)*, vol. 174, pp. 455-460, 2011.

[28] S. Sugimoto, R. Segawa, D. Noguchi, Y. Bannai, and K. Okada, "Presentation technique of scents using mobile olfactory display for digital signage," in *13th IFIP TC 13 International Conference on Human-Computer Interaction, INTERACT 2011, September 5, 2011 - September 9, 2011*, Lisbon, Portugal, 2011, pp. 323-337.

[29] Y. Yanagida, S. Kawato, H. Noma, A. Tomono, and N. Tesutani, "Projection based olfactory display with nose tracking," in *IEEE Virtual Reality 2004, 27-31 March 2004*, Piscataway, NJ, USA, 2004, pp. 43-50.

[30] D. W. Kim, K. Nishimoto, S. Kunifuji, Y. H. Cho, Y. Kawakami, and H. Ando, "Development of aroma-card based soundless olfactory display," in *2009 16th IEEE International Conference on Electronics, Circuits and Systems, ICECS 2009, December 13, 2009 - December 16, 2009*, Yasmine Hammamet, Tunisia, 2009, pp. 703-706.

[31] T. Nakamoto, H. Takigawa, and T. Yamanaka, "Fundamental study of odor recorder using inkjet devices for low-volatile scents," *IEICE Transactions on Electronics,* vol. E87-C, pp. 2081-6, 2004.

[32] Y. Ariyakul and T. Nakamoto, "Olfactory display using a miniaturized pump and a SAW atomizer for presenting low-volatile scents," in *2011 IEEE Virtual Reality (VR), 19-23 March 2011*, Piscataway, NJ, USA, 2011, pp. 193-4.

[33] T. Nakamoto and K. Murakami, "Selection method of odor components for olfactory display using mass spectrum database," in *2009 IEEE Virtual Reality Conference, 14-18 March 2009*, Piscataway, NJ, USA, 2009, pp. 159-62.

[34] T. Tanikawa, A. Nambu, T. Narumi, K. Nishimura, and M. Hirose, "Olfactory display using visual feedback based on olfactory sensory map," in *4th International Conference on Virtual and Mixed Reality, Held as Part of HCI International 2011, July 9, 2011 - July 14, 2011*, Orlando, FL, United states, 2011, pp. 280-289.

[35] J. A. Gottfried and R. J. Dolan, "The Nose Smells What the Eye Sees:: Crossmodal Visual Facilitation of Human Olfactory Perception," *Neuron,* vol. 39, pp. 375-386, 2003.

[36] *Spraying Systems Co. Catalog 70* [Internet]. Available: http://www.spray.com/cat70/index.aspx

[37] *Fluent 6.2 Documentation*. Available: http://www.ansys.com/

[38] W. Jones and B. E. Launder, "The prediction of laminarization with a two-equation model of turbulence," *International Journal of Heat and Mass Transfer,* vol. 15, pp. 301-314, 1972.

[39] R. W. Fox, A. T. McDonald, and P. J. Pritchard, *Introduction to Fluid Mechanics*, 6 ed. Hoboken, NJ: Wiley, 2004.

[40] R. P. Canale and S. C. Chapra, *Numerical Methods for Engineers*, 5 ed. New York, NY: McGraw-Hill, 2006.

[41] J. C. Chang, S. R. Hanna, Z. Boybeyi, and P. Franzese, "Use of Salt Lake City URBAN 2000 field data to evaluate the urban Hazard Prediction Assessment Capability (HPAC) dispersion model," 2010.

[42] W. S. Cain, "Testing olfaction in a clinical setting," *Ear, nose, & throat journal*, vol. 68, pp. 316, 322-8, 1989 1989.

[43] T. Hummel, B. Sekinger, S. R. Wolf, E. Pauli, and G. Kobal, "'Sniffin' sticks': olfactory performance assessed by the combined testing of odor identification, odor discrimination and olfactory threshold," *Chemical senses*, vol. 22, pp. 39-52, 1997 1997.